ISTITUTO ITALIANO DI TECNOLOGIA
CENTER FOR NANOSCIENCE AND TECHNOLOGY

The key enabling role of ductile amorphous oxide coatings for GIV and fusion nuclear power plants.

B. Paladino[1,2], M. Cabrioli[1,2], A. Stinchelli[1,2], S. Bassini[3], M. Utili[3], M. Angiolini[3], M. Tarantino[3], P. Agostini[3], F. Di Fonzo[1].

[1]Center for Nano Science and Technology@PoliMi, Istituto Italiano di Tecnologia, Milano, Italy

[2]Dipartimento di Energia, Politecnico di Milano, Milano, Italy

[3]ENEA FSN Department, C.R. Brasimone, Camugnano (Bo), Italy

ISTITUTO ITALIANO DI TECNOLOGIA
CENTER FOR NANOSCIENCE AND TECHNOLOGY

Why next generation nuclear systems need coatings and the key enabling role of ductile amorphous oxide coatings for GIV and fusion nuclear power plants.

B. Paladino[1,2], M. Cabrioli[1,2], A. Stinchelli[1,2], S. Bassini[3], M. Utili[3], M. Angiolini[3], M. Tarantino[3], P. Agostini[3], F. Di Fonzo[1].

[1]Center for Nano Science and Technology@PoliMi, Istituto Italiano di Tecnologia, Milano, Italy

[2]Dipartimento di Energia, Politecnico di Milano, Milano, Italy

[3]ENEA FSN Department, C.R. Brasimone, Camugnano (Bo), Italy

➢ Next generation nuclear systems benefits:

- **increasing efficiency** (higher cycle temperature)
- **reducing waste generation** (burning effect)
- **enhancing safety** (passive systems, new coolants, etc.)
- **promoting non-proliferation** (closed fuel cycle)

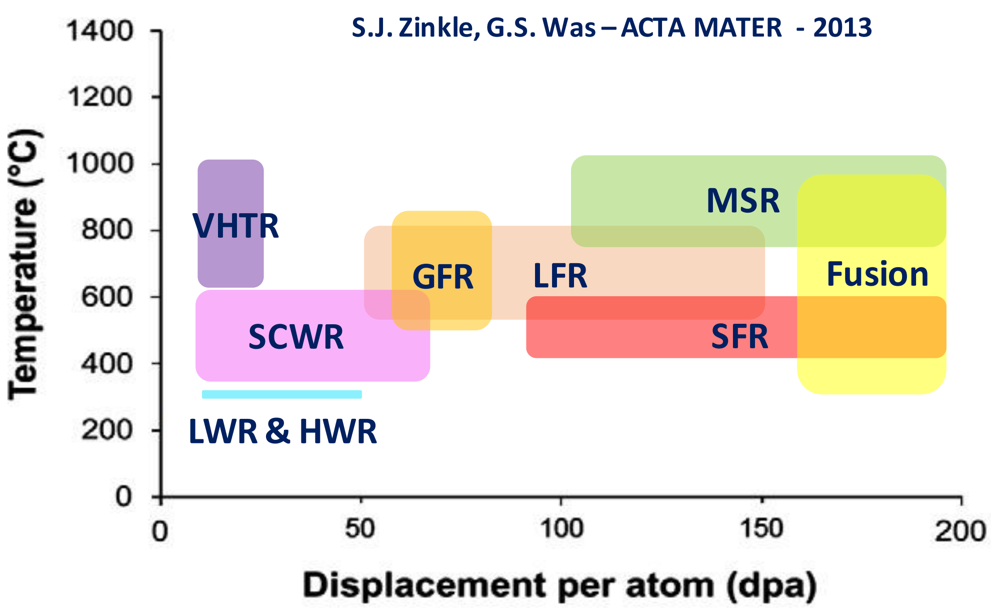

FISSION REACTORS:

LWR: Light Water Reactor
HWR: Heavy Water Reactor

~~GII and GIII present reactors~~

SCWR: Supercritical Water Reactor
VHTR: Very High T Reactor
GFR: Gas-cooled Fast Reactor
LFR: Lead-cooled Fast Reactor
SFR: Sodium-cooled Fast Reactor
MSR: Moten Salts Reactor

Gen IV (GIV) reactors

FUSION REACTORS

fabio.difonzo@iit.it

Future generation nuclear systems aim at:

- **Increase efficiency**
- **Reduce waste generation**
- **Enhance safety**
- **Promote non-proliferation**

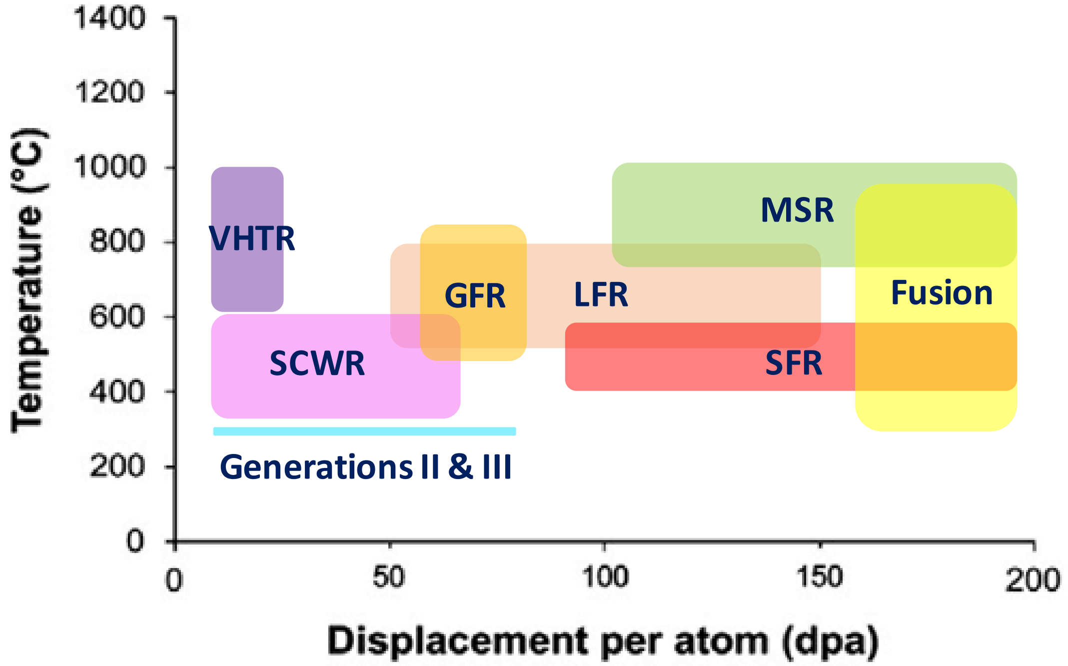

S.J. Zinkle and G.S. Was – Acta Materialia - 2013

Ultimate goal for LFRs:

- **800 °C**
- **150 dpa**

Advantages:

safety
transmutation of minor actinides / fuel breeding

Major issues:

- **corrosion**
- **radiation damage**
- **Tritium permeation**

S.J. Zinkle and G.S. Was – Acta Materialia - 2013

Future generation nuclear systems impose

Tritium management

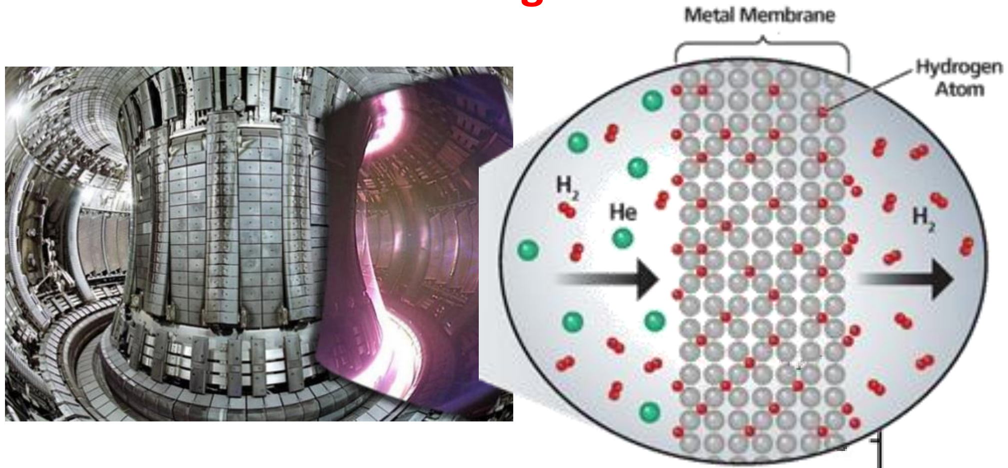

Corrosion

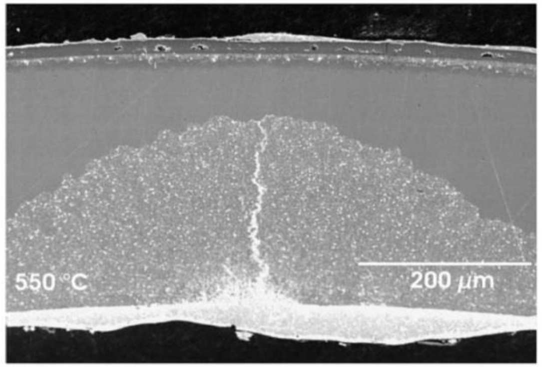

G. Mueller et al. – J Nucl Mater – 2004

Radiation damage

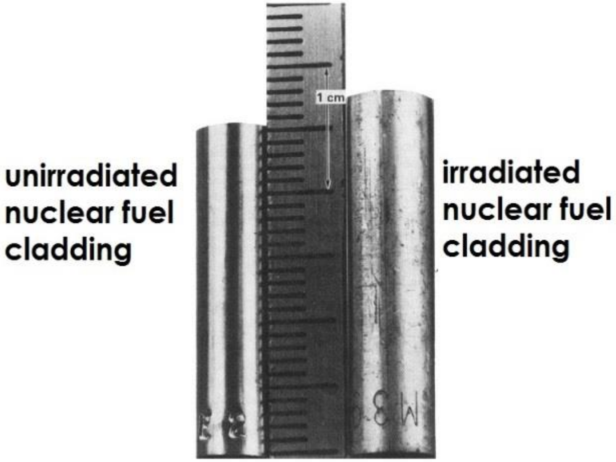

J.L. Straalsund – Westinghouse Hanford

Magnetohydrodynamics, MHD

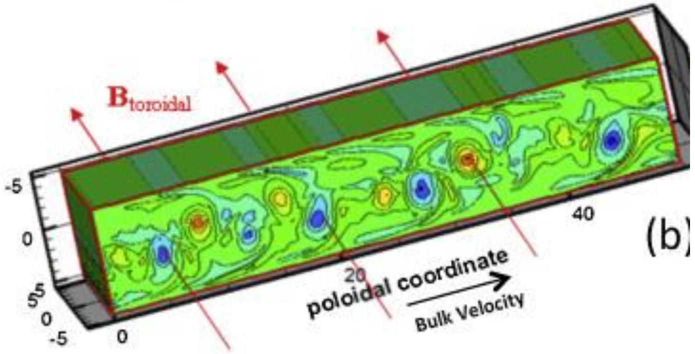

M. Abdou et al. Fus Eng.&Des 2015

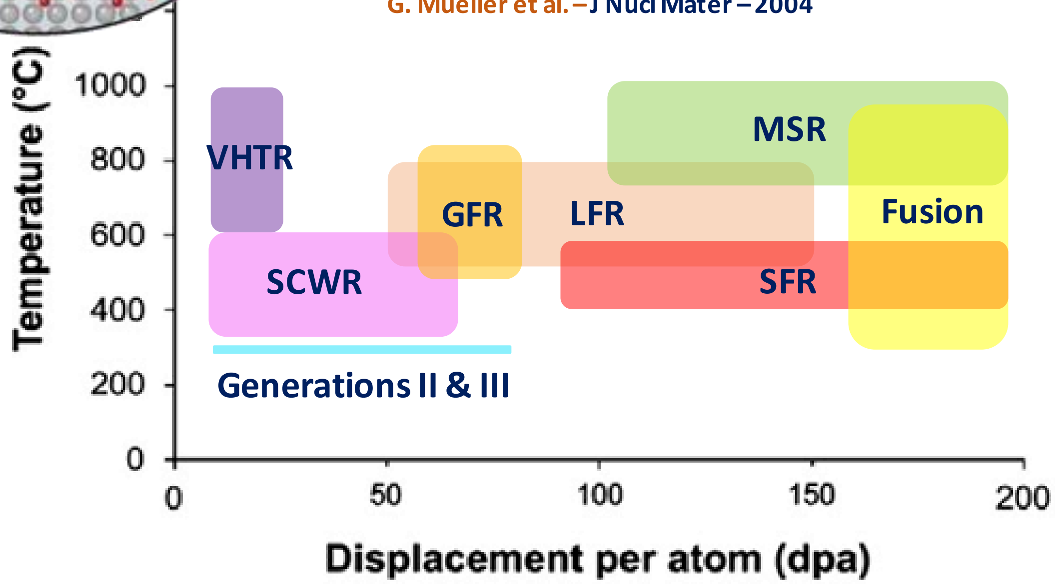

S.J. Zinkle and G.S. Was – Acta Materialia - 2013

MAJOR BOTTLENECKS FOR ALL SYSTEMS

NEED FOR COATINGS

Tritium permeation
(radiological hazard, loss of fuel)

Tritium in fission

Tritium production rates of different fission reactors (*) :

Reactor type	Total tritium source term (TBq.GWe^{-1}.year^{-1})	Tritium transferred into coolant (TBq.GWe^{-1}.year^{-1})
PWR	567	37
BWR	520	much lower than PWR (no boric acid)
GCR (MAGNOX)	705	very small due to Mg cladding
PHWR (CANDU)	54170	53650 **(up to 90000)**
SFR	3034	1000

- in PWR tritium produced in fuel pins keeps occluded (affinity with Zr, limited permeation in ZrO_2)
- in SFR, stainless steel claddings (high T) is totally permeable to tritium

Tritium management is an important issue in SFR

*(*) **average** data from IRSN report and ASN report (« Livre blanc du tritium »)*

Since 2000, **PWR cover ≈ 65%** of worldwide **electrical power production**

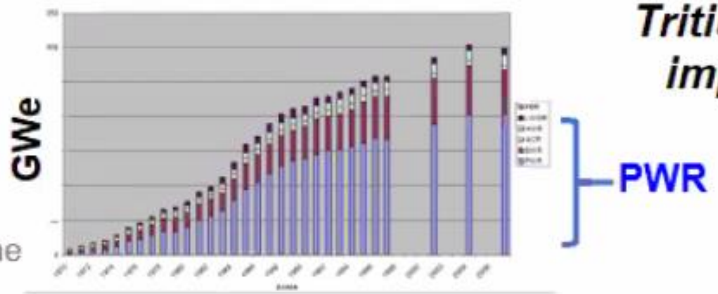

T. Gilardy, 2nd Tritium School, 2021

Tritium in SFR

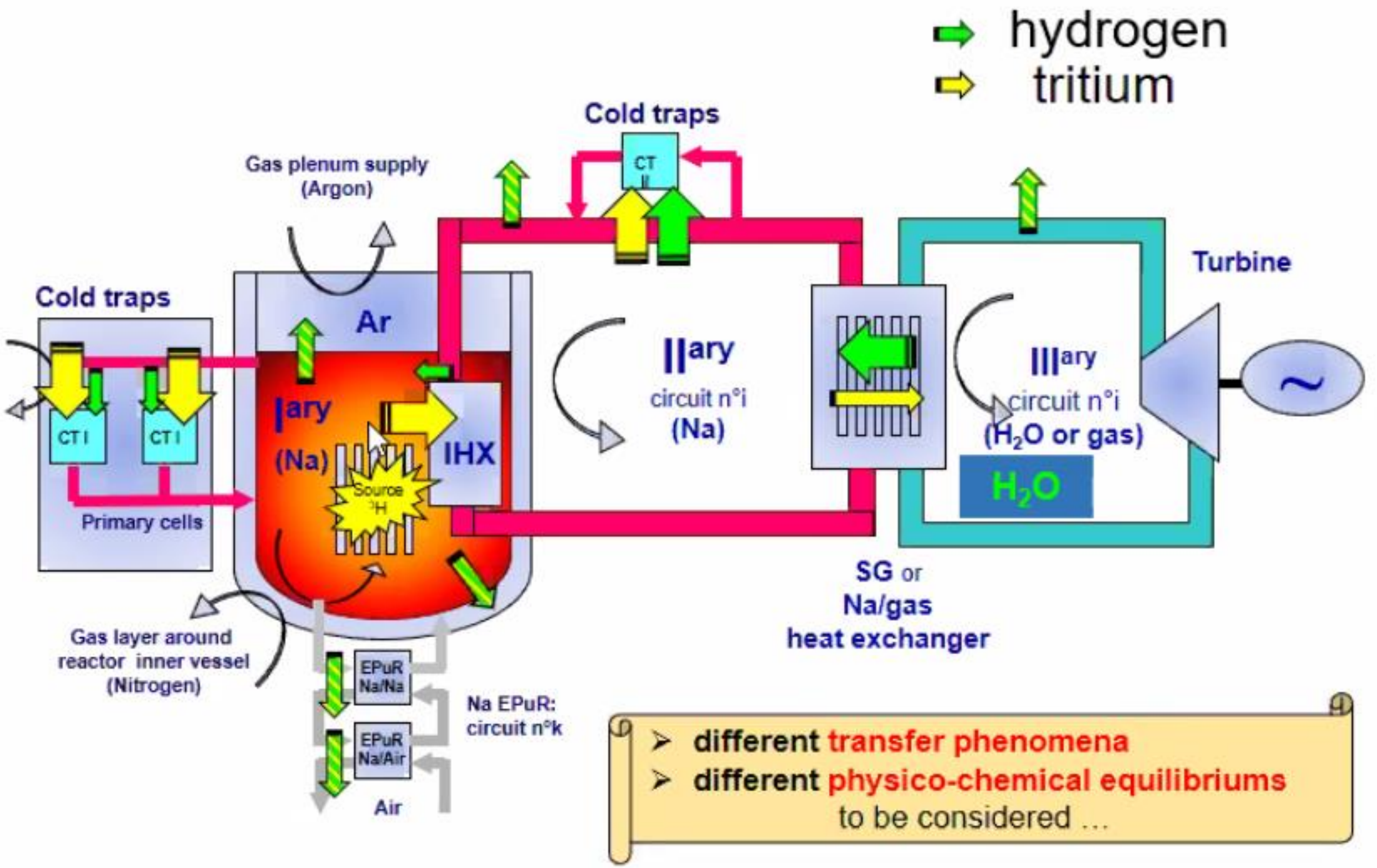

T. Gilardy, 2nd Tritium School, 2021

Tritium in fusion: mitigation strategies are essential

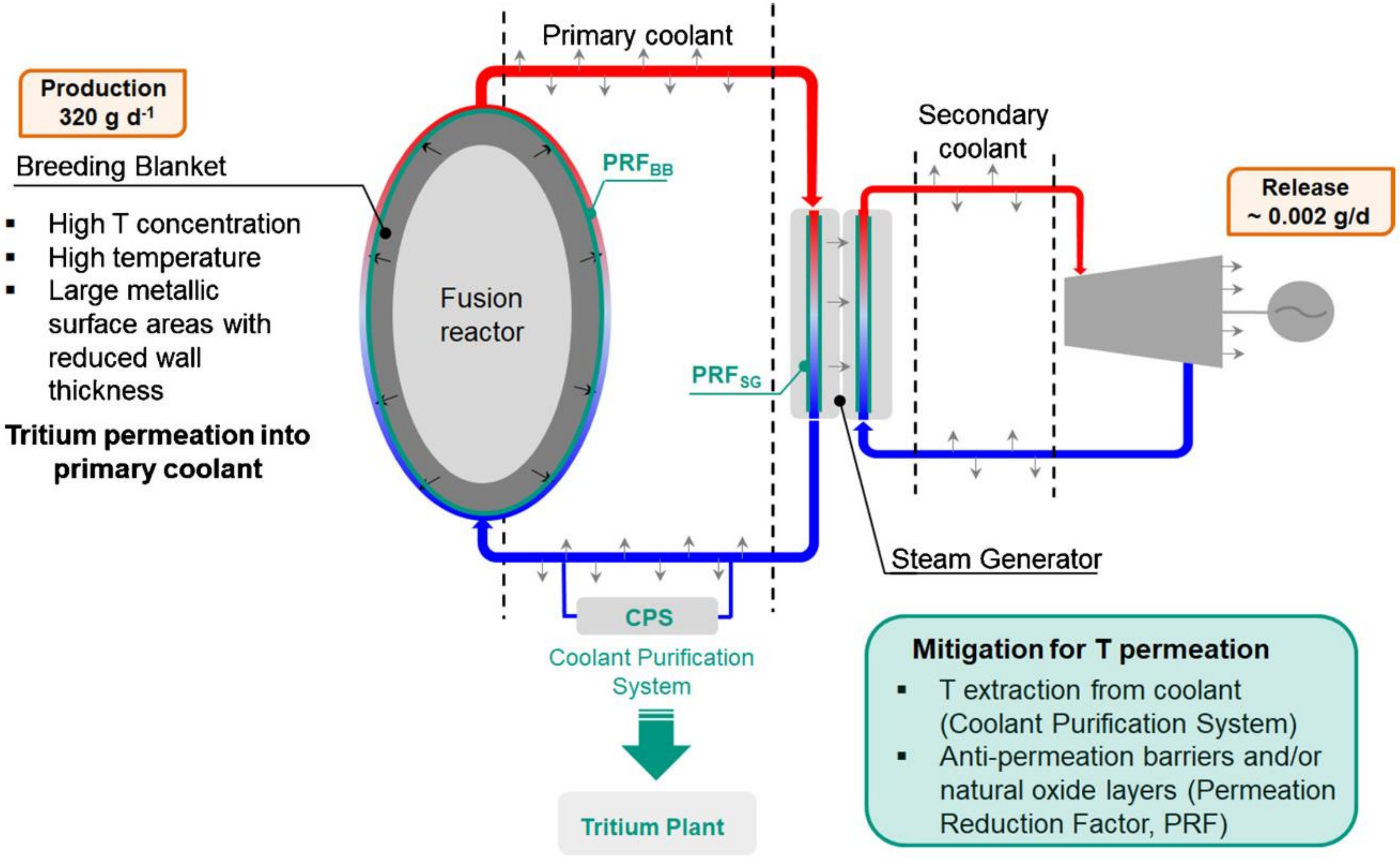

Fig. 1. Generic view of the tritium migration path in DEMO coolant.

- Mandatory limit of 0,002 g/d (less than 1 g/y) of tritium release
- T release without any mitigation strategies: HCPB ≈ 1 g/d & WCLL ≈ 37 g/d (respectively 0,35 % and 11 % of the T produced in the blanket)
- **No fusion power plant can be built without suppressing the permeation of tritium**

Mechanics of tritium transport

- The basic processes to be studied in a circuit consists of three domains: Liquid Metal, Solid, Gas.

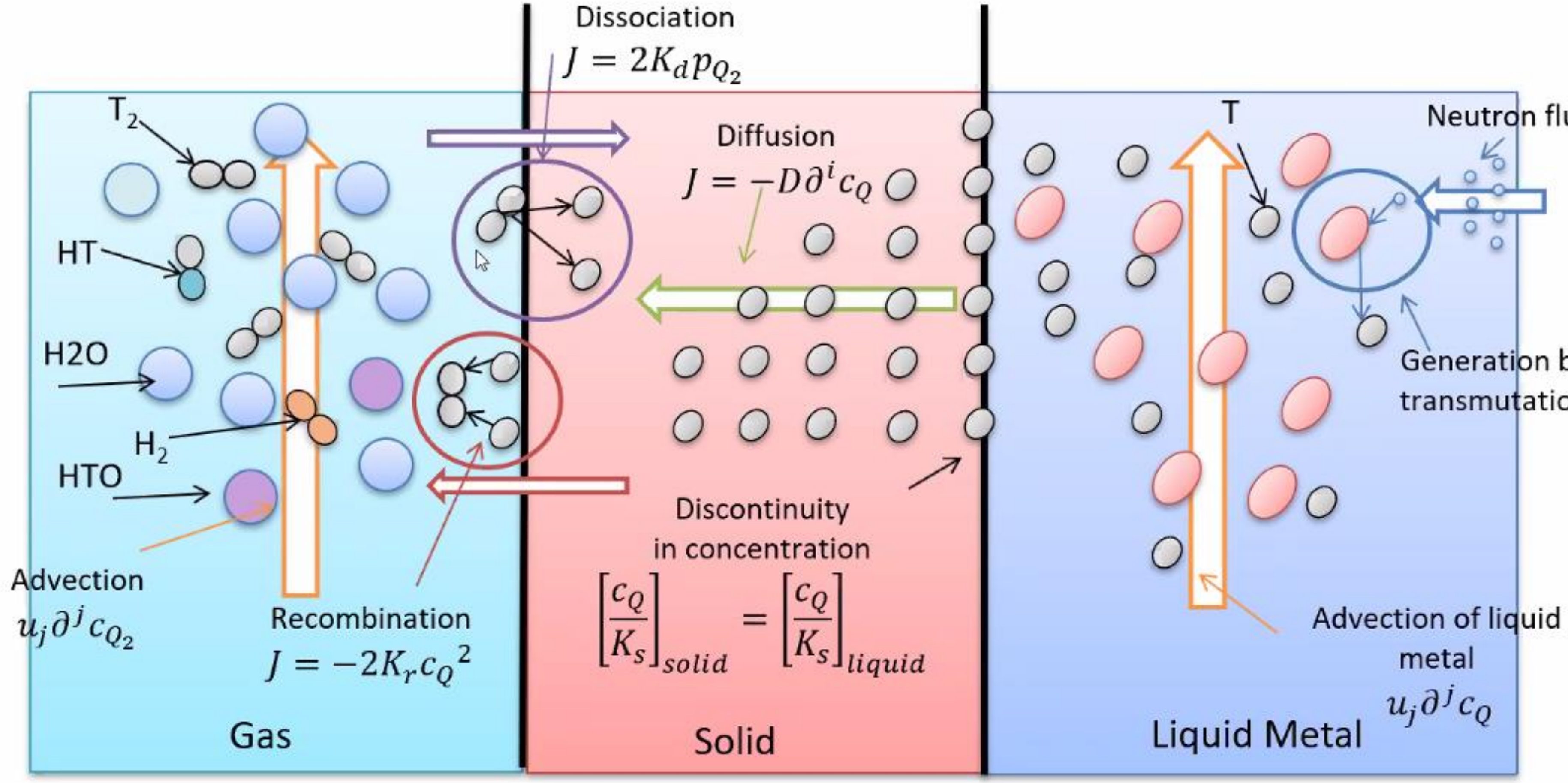

C. Moreno, 2nd Tritium School, 2021

The permeation barriers

Apply a barrier on all the surfaces where high tritium permeation fluxes are expected

- The main parameter to take in account is the Permeation Reduction Factor (PRF), which is the ability of the coating to suppress permeation
- The PRF depends on the operative temperature, on the material, and on the number of defects present in the coating
- A PRF value above 1000 (at 450 °C) is necessary to satisfy the limit in tritium release
- Protective barriers also useful for corrosion protection of the strucutural steels of for suppression of MHD effects

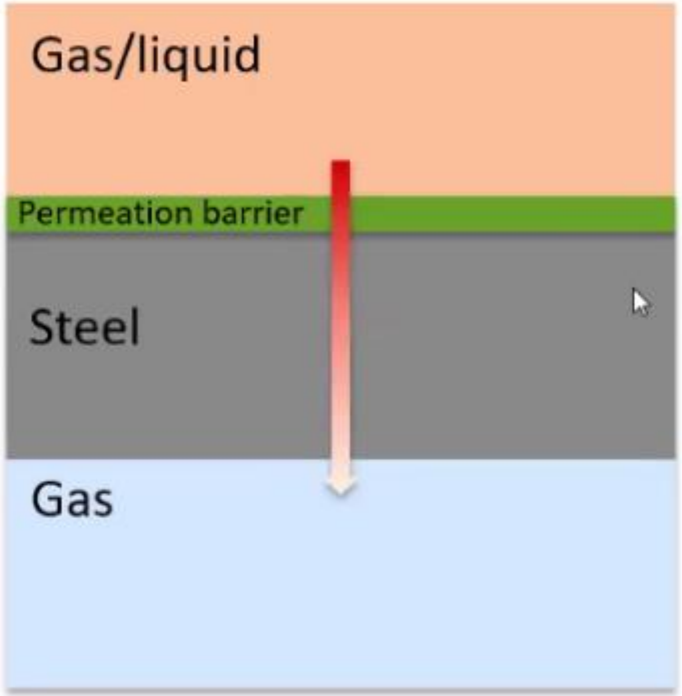

$$PRF = \frac{J_{uncoated}}{J_{coated}}$$

PB effect in WCLL (C. Moreno, 2nd Tritium School)

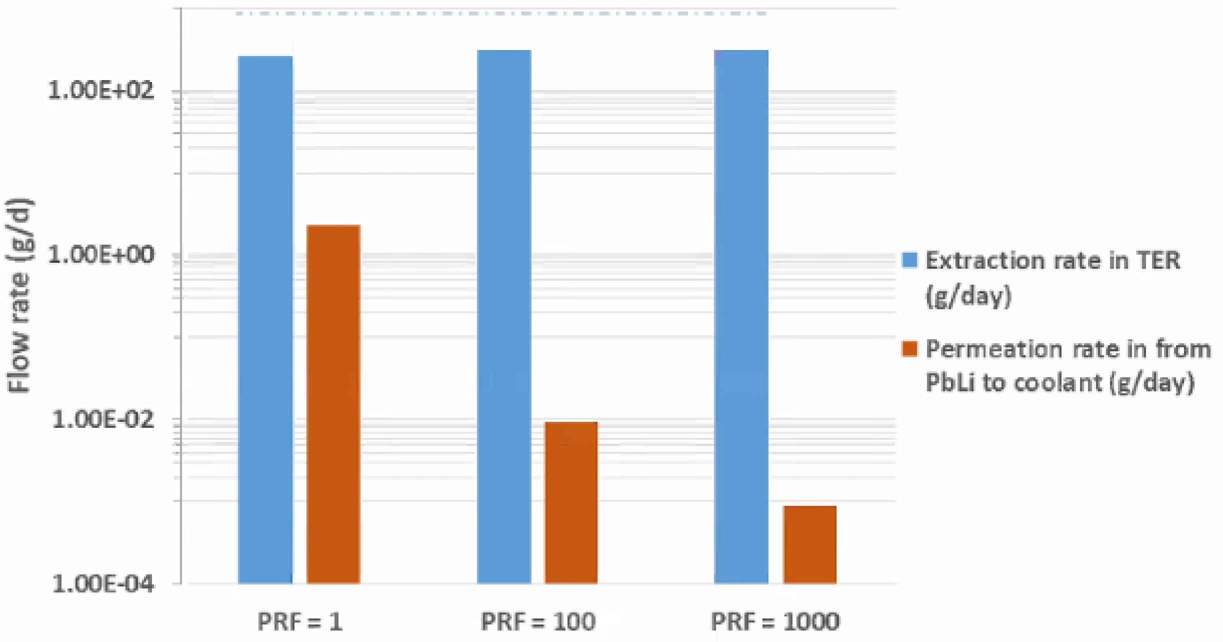

Values after 5 years.

Inventories in coolant decrease as PRF is increased.

It can be noticed how the reduction in the permeation rates increases slightly the concentration in PbLi but reduces very significantly the concentration in the water circuits.

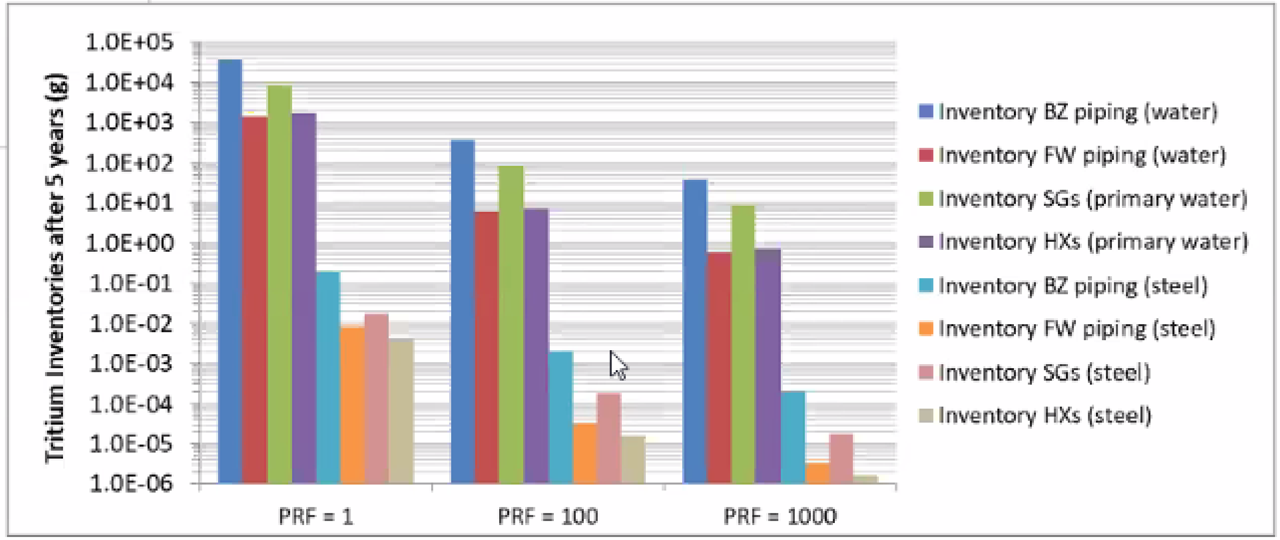

ISTITUTO ITALIANO
DI TECNOLOGIA

HLM Corrosion Mitigation Strategies

Ni leaching in austenitics (23000 h @ 550°C, 10^{-6} wt.% O)

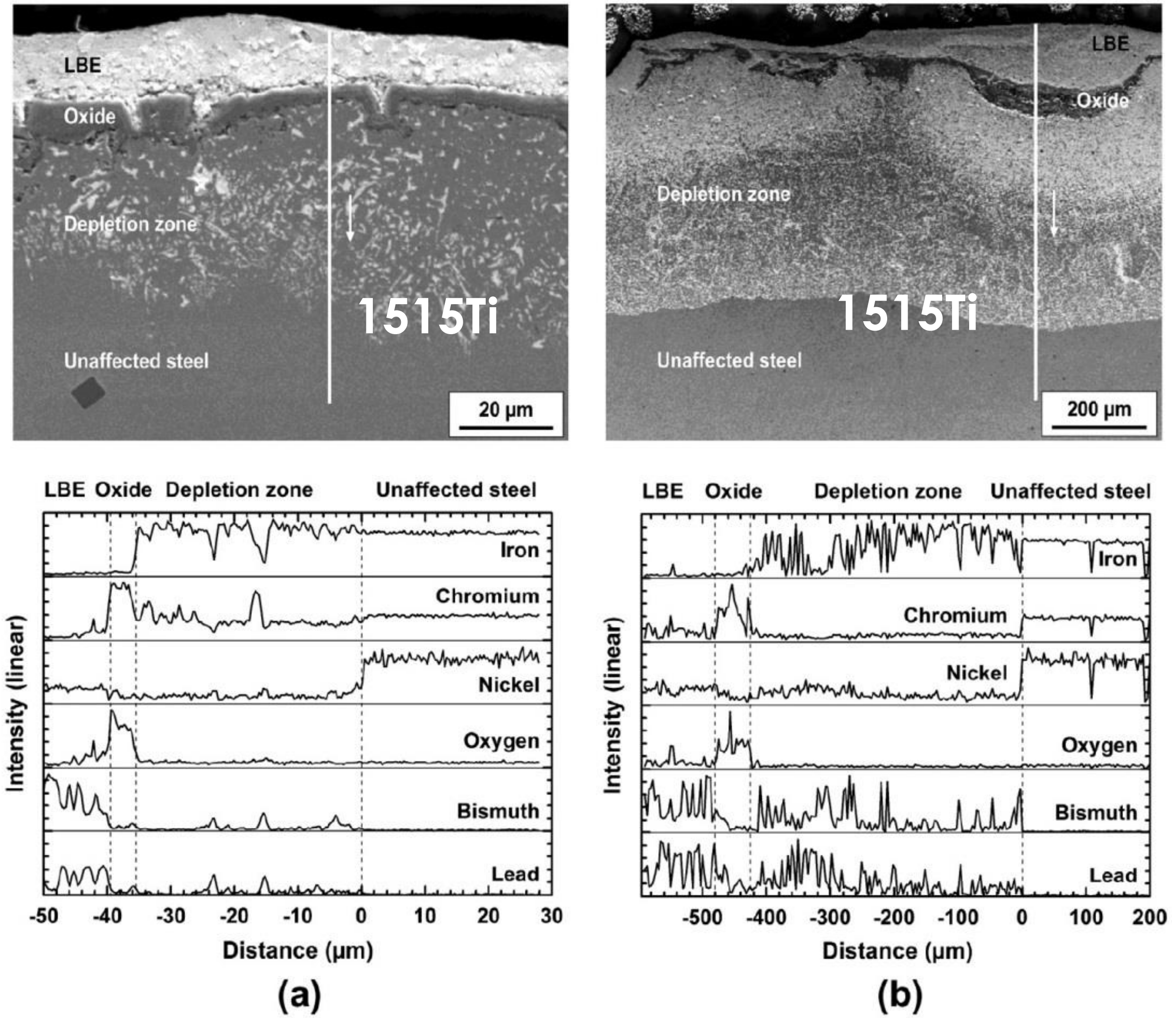

C. Schroer et al. - Corros. Sci. - 2014

Solubility of Ni in lead is very high

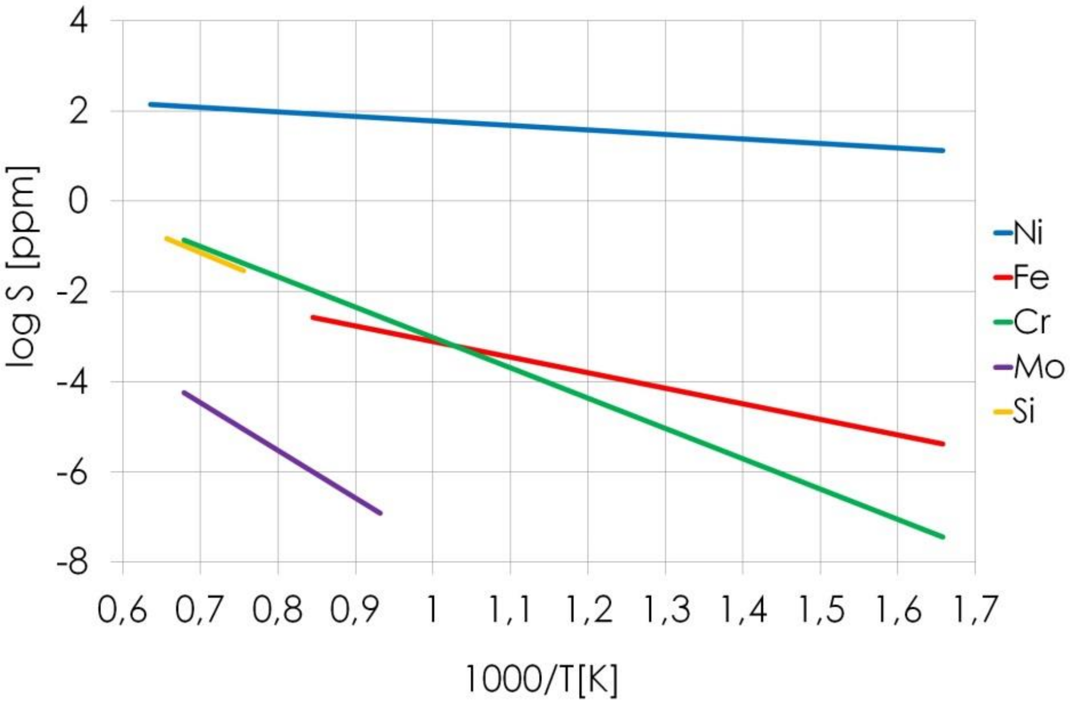

Heavy liquid metal corrosion

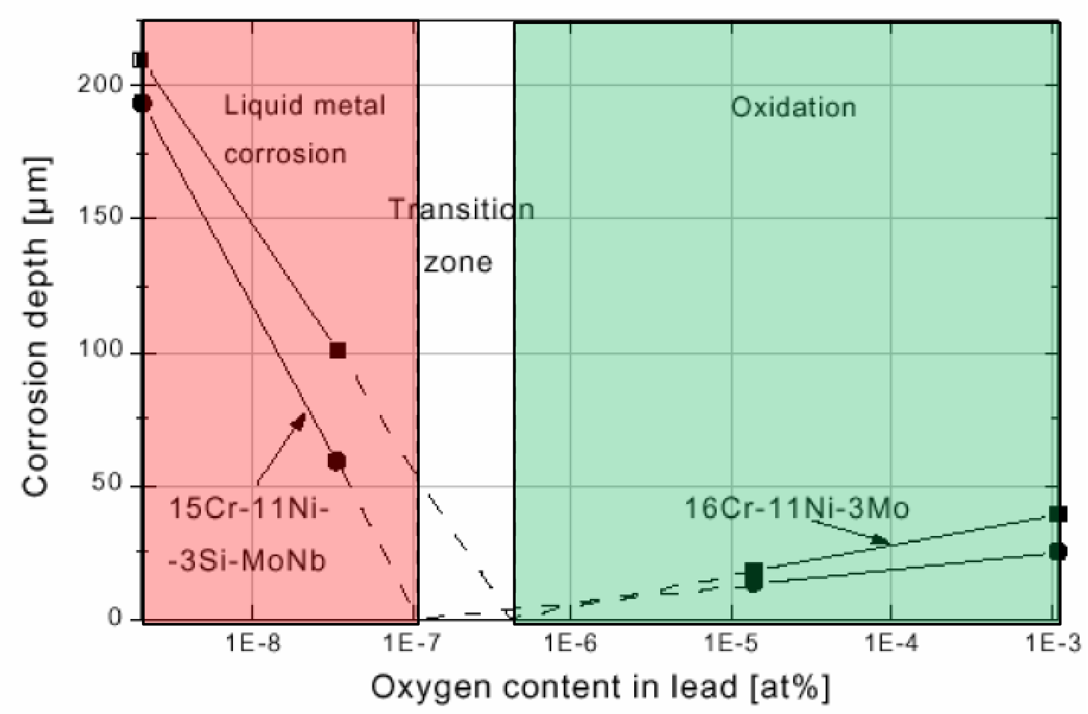

Austenitic steels exposed to HLM for 3000 hours at 550°C

V. Gorynin et al. – Metal Science and Heat Treatment - 1999

G. Mueller et al. – J Nucl Mater – 2004

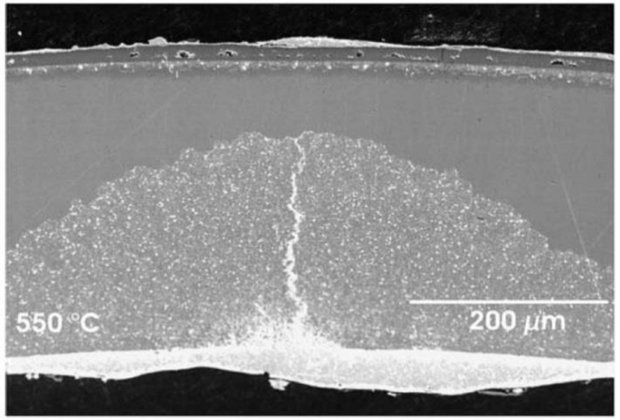

Dissolution

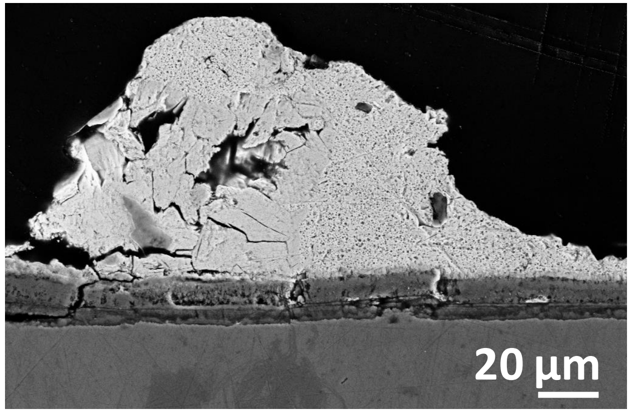

Oxidation

In-situ passivation is not viable for T > 500°C (will be exceeded by fuel cladding)

Impact of temperature (1st stage)

Margin to lead-oxide formation
(to avoid risk of plugging)

Sufficient margin
(to guarantee control)

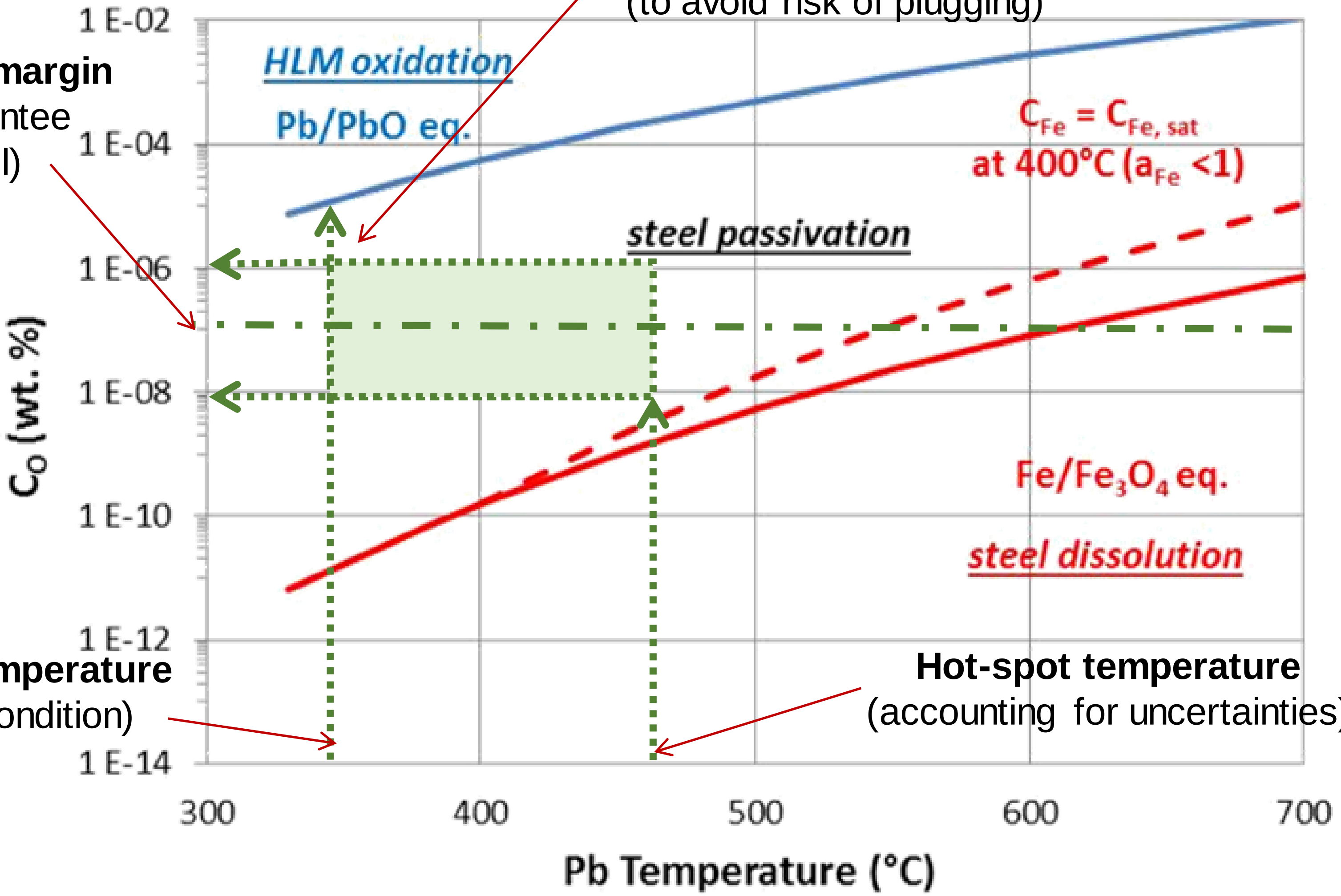

Lowest temperature
(in any condition)

Hot-spot temperature
(accounting for uncertainties)

Impact of temperature (final stage)

Same O2 control window

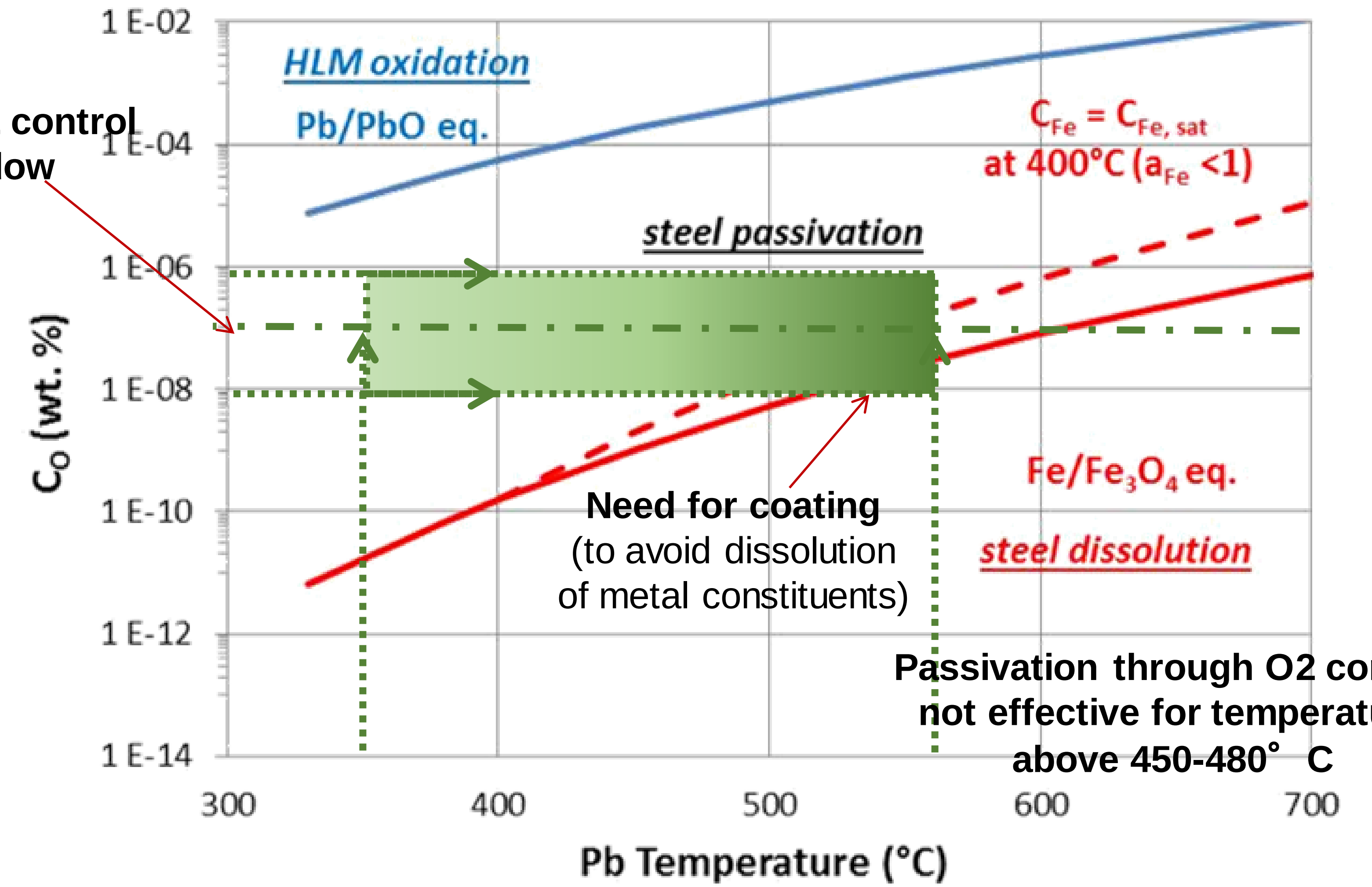

Need for coating
(to avoid dissolution of metal constituents)

Passivation through O2 control not effective for temperature above 450-480° C

Lead Fast Reactor - ALFRED

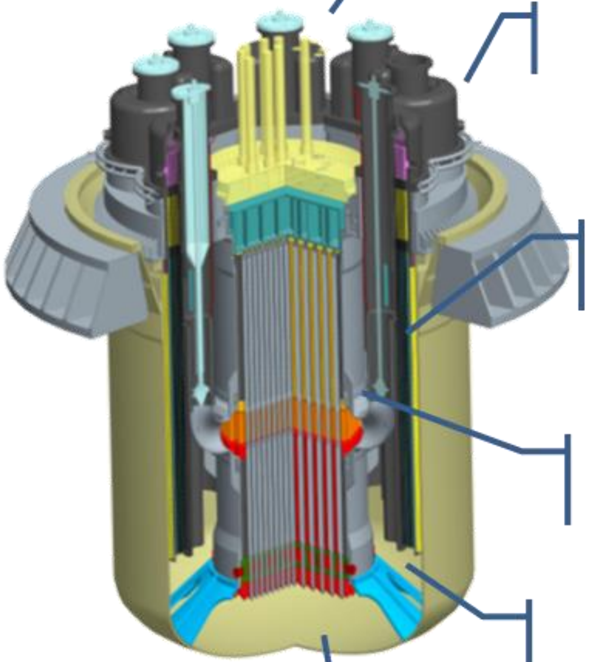

Relatively low power (300 MWth)

Compact design
Removable components
Proven technologies

Simple flow path
Efficient natural circulation

Inner vessel
Enclosing hot pool

Molten lead as coolant
Excellent intrinsic properties
Manageable negative properties

Pool-type Primary System

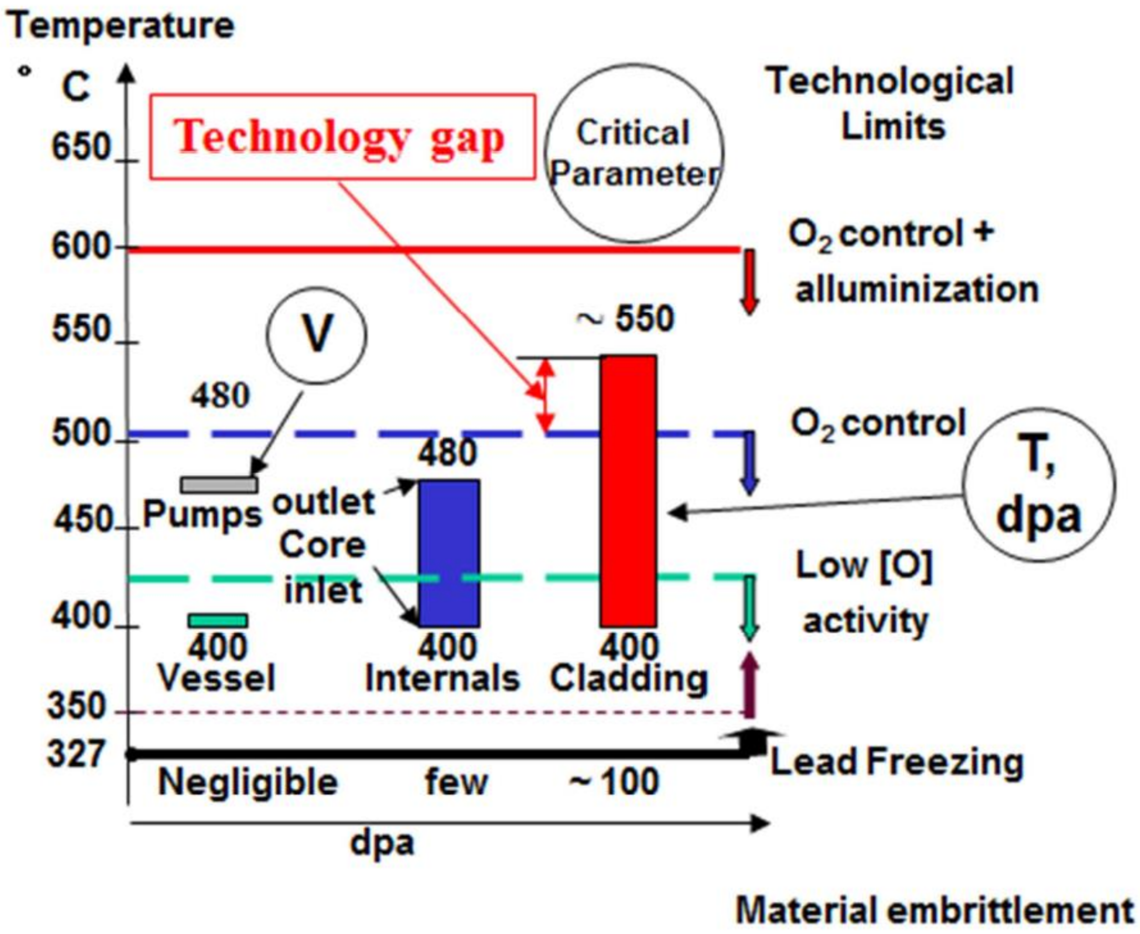

- **Pb-Li based Breeding Blanket (BB)**
  - first wall **heat removal**
  - **neutron moderator/multiplier** (thanks to Pb)
  - **tritium breeder** through **nuclear transmutations**

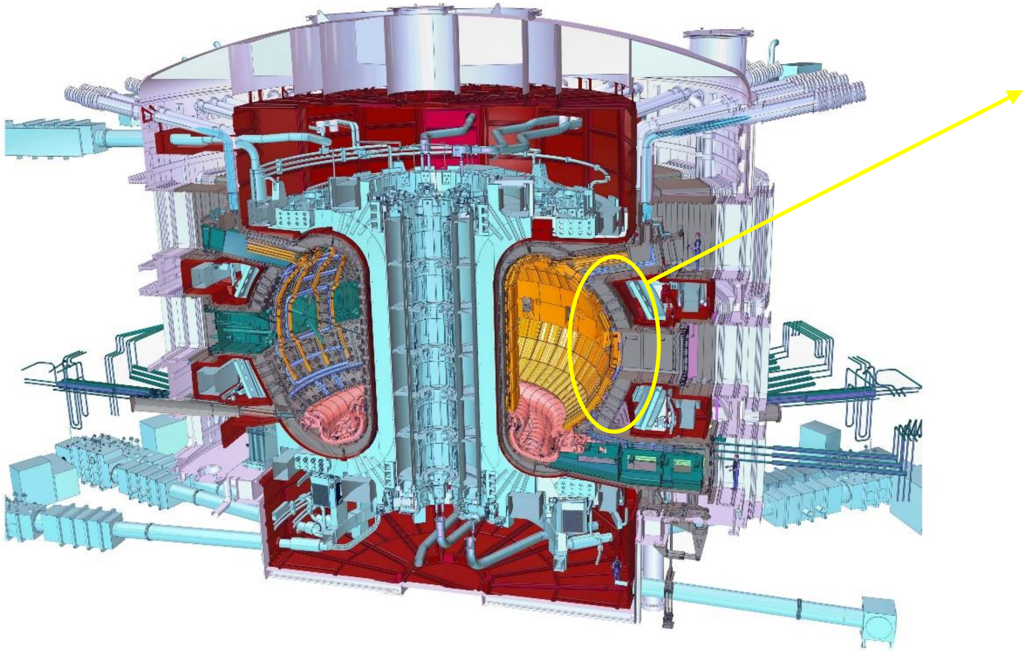

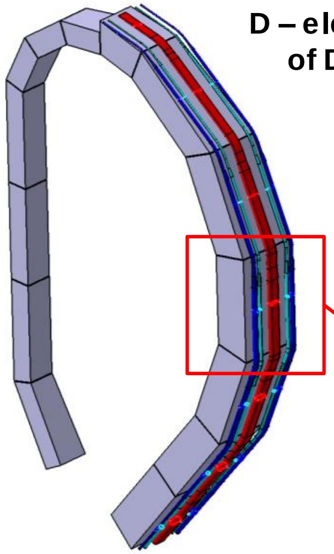

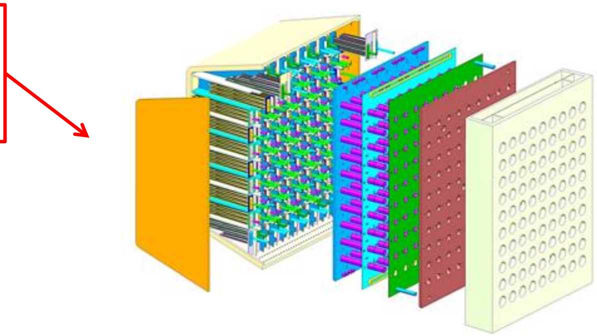

- **Working conditions for fusion:**
  - **up to 200 dpa**
  - **450 – 550 °C**
  - **NO SUITABLE MATERIALS**

fabio.difonzo@iit.it

➢ HLM corrosion operated by lead-lithium eutectic (LLE): the combined action of Pb and Li

Corrosion rates in pure Li VS Pb-Li

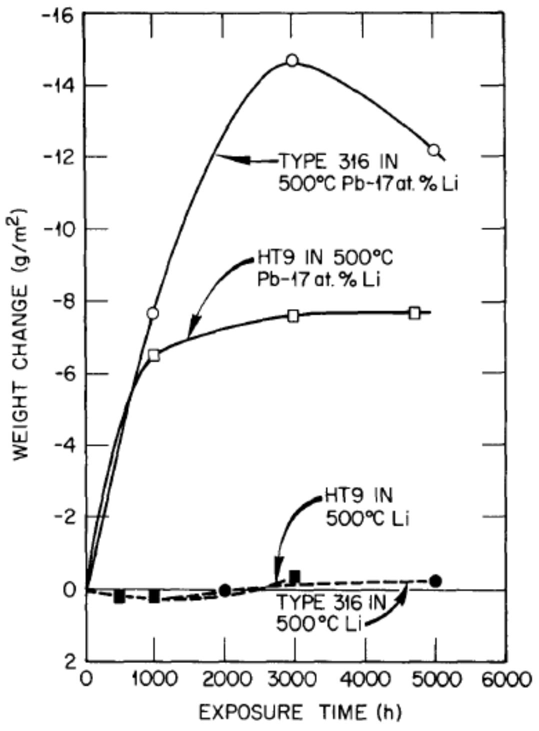

P.F. Tortorelli et al. – J MATER ENERG SYST – 1982

Thermo-dinamical potential of Pb-Li VS different oxides

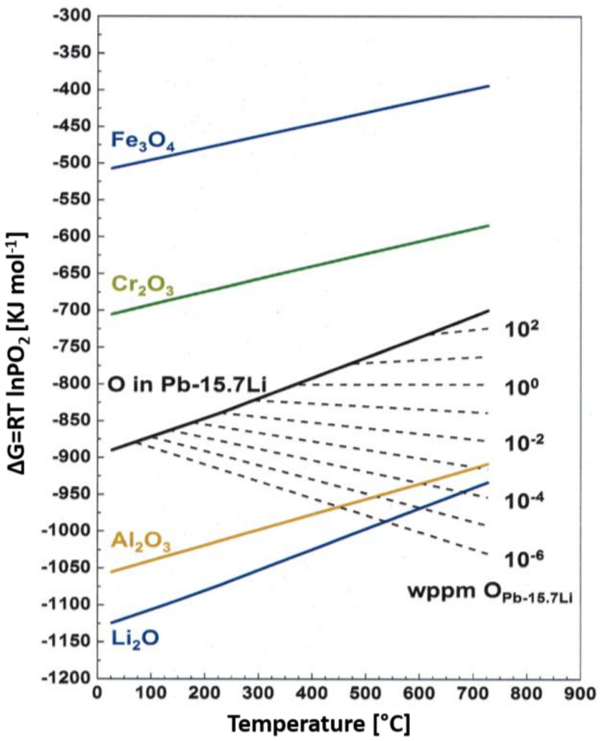

Credits to S. BASSINI from ENEA

⟹ **Lithium presents high affinity with oxygen: it tends to reduce (any) metal oxides, depending on the conditions**

Coatings for nuclear applications

Requirements for environmental barrier coatings for structural materials in fission (fuel cladding, core components) and fusion (BB)

Mechanical performance

Ductility, hardness, strength

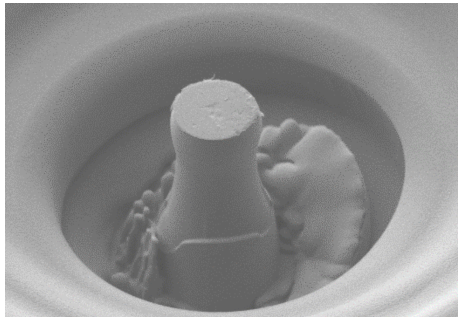

$H_2/D_2/T_2$ permeation

Amorphous structure

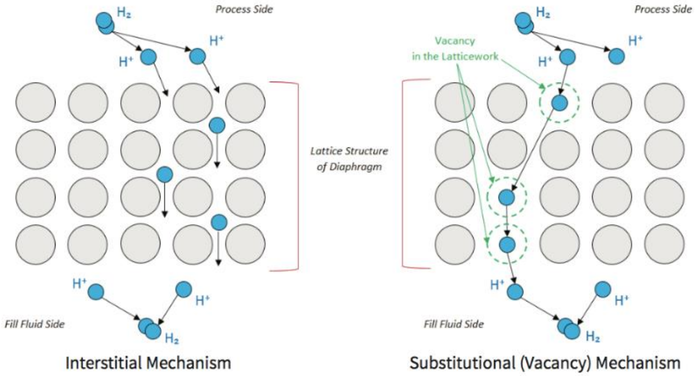

Corrosion resistance

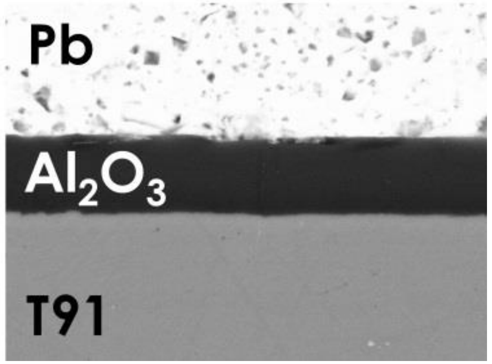

Radiation tolerance

Interstitial emission from GBs

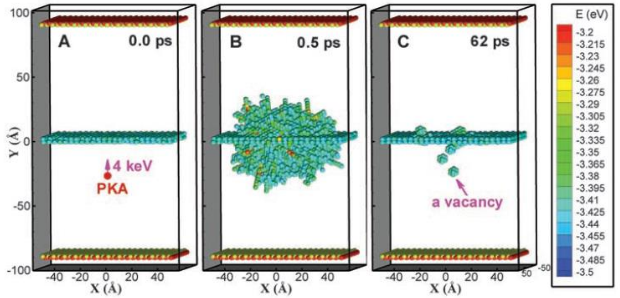

X.M. Bai et al. – Science - 2010

Thin films in fusion

Table 2
State of the art efficiency of some selected dielectric materials, recently recognised as HPBs, expressed as P_f at 400 °C.

	PRF	d_s mm	d_f μm	P_s x10^{-11} molH$_2$/s/m/Pa$^{0.5}$	P_f x10^{-18} molH$_2$/s/m/Pa$^{0.5}$	Ref
Al_2O_3	1000	0.5	1	1.30	25.9	29
Cr_2O_3	1000	1.6	10*	0.017	0.72*	31
Cr_2O_3/Al_2O_3	3500	0.5	1	1.30	7.41	34
Er_2O_3	1000	0.5	1	1.30	25.9	35
Er_2O_3	1000	0.5	1.3	1.30	33.7	36
SiO_2	1	0.15	0.2	0.13	1711	40
BN	100	0.1	1.5	0.13	193	42
TiN	100	0.1	1.5	0.13	193	42
TiN	1100	0.35	1.7	0.13	5.7	43
TiN	1000	0.1	1.7	0.13	21.8	43
TiAlN	6800	0.35	1.7	0.13	0.92	44
TiAlN	20,000	0.5	5	1.30	6.5	45
SiN	2000	0.5	0.5	1.30	6.5	25
WN	38	0.5	2.3	1.30	1570	48
CrWN	100	0.5	4.4	1.30	1140	48
CrN	117	0.5	2.6	1.30	576	48
Cr_2N	236	0.5	2.2	1.30	241	48
AlCrN	350	0.5	4.5	1.30	333	48
ZrN	4600	0.5	1.4	1.30	7.9	48
TiC	10	0.1	1	0.27	2750	52
TiN + TiC	100	0.5	1 + 0.25	1.30	324	53

V. Nemanič   Nuclear Materials and Energy 19 (2019) 451–457

INTERNATIONAL JOURNAL OF HYDROGEN ENERGY 41 (2016) 10374–10379
Available online at www.sciencedirect.com
ScienceDirect
journal homepage: www.elsevier.com/locate/he

Influence of annealing atmosphere on the deuterium permeation of Y_2O_3 coatings

Wu Yunyi*, Shuai Li, Di He, Xiaopeng Liu, Shumao Wang, Lijun Jiang

Yttria deposited by **MOCVD + annealing 700 °C.**

As prepared / After permeation test

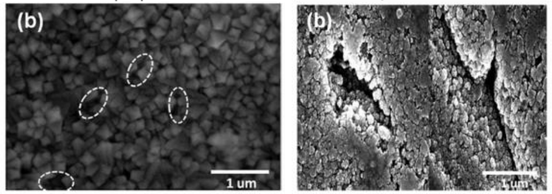

Table 1 – The PRF values of the coating S2 in the first and second permeation measurement cycles.

Temperature (°C)	500	550	600	650	700
First cycle	412	332	242	181	102
Second cycle	276	197	131	87	43

Fusion Engineering and Design 133 (2018) 121–124
Contents lists available at ScienceDirect
Fusion Engineering and Design
journal homepage: www.elsevier.com/locate/fusengdes

Deuterium permeation through monoclinic erbium oxide coating

Takumi Chikada[a,*], Hikari Fujita[b], Masayuki Tokitani[c], Yoshimitsu Hishinuma[c], Takayuki Terai[b], Yasuhisa Oya[a]

Erbia deposited by **vacuum arc vapor deposition (1.3–1.6 μm).**
The substrate temperature was @ **600 °C**

As deposited

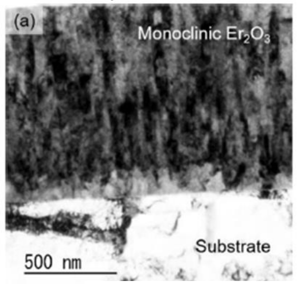

MAX PRF ≈ 1000 @ 700 °C

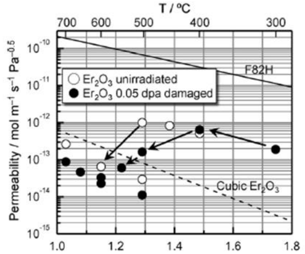

Surface & Coatings Technology 205 (2011) 2709–2713
Contents lists available at ScienceDirect
Surface & Coatings Technology
journal homepage: www.elsevier.com/locate/surfcoat

Hydrogen permeation through TiAlN-coated Eurofer '97 steel

Paul J. McGuiness[a,*], Miha Čekada[b], Vincenc Nemanič[c], Bojan Zajec[c], Aleksander Rečnik[a]

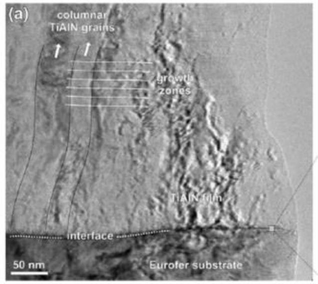

Deposition using four unbalanced **DC magnetron** sources. Targets: **bulk titanium with aluminium plugs**. Total thickness of **5 μm** (2 μm/h). The deposition temperature was about **450 °C**.

MAX PRF = 20000 @400 °C. After 10 days the PRF dropped to 5800

Surface & Coatings Technology 202 (2008) 5043–5047
Contents lists available at ScienceDirect
Surface & Coatings Technology
journal homepage: www.elsevier.com/locate/surfcoat

Al–Cr–O thin films as an efficient hydrogen barrier

Denis Levchuk[a], Harald Bolt[a], Max Döbeli[b], Simon Eggenberger[c], Beno Widrig[c], Jürgen Ramm[c,*]

Coatings by **cathodic arc evaporation@** T = **550 °C**, thickness **1 μm**.

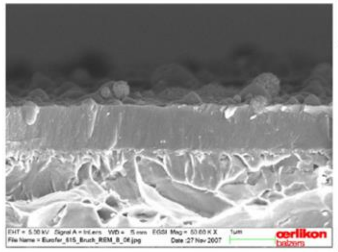

MAX PRF = 3500 @700 °C

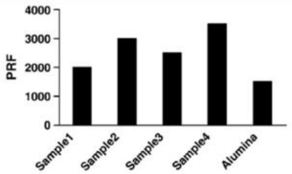

Fig. 4. The measured mean PRF values for the investigated samples. For comparison, data of a 1 μm thick alumina film deposited at 720 °C from [4] is given.

ECA - ECX methods

Electrochemical processes:
- **ECA** (organic electrolyte)
- **ECX** (Ionic liquids)

The formation of the functional surface requires specific heat treatments:
- 913K/4h in Air/Ar
- 1253K/0.5h + 1033K/1.5h in air
- Natural cooling down

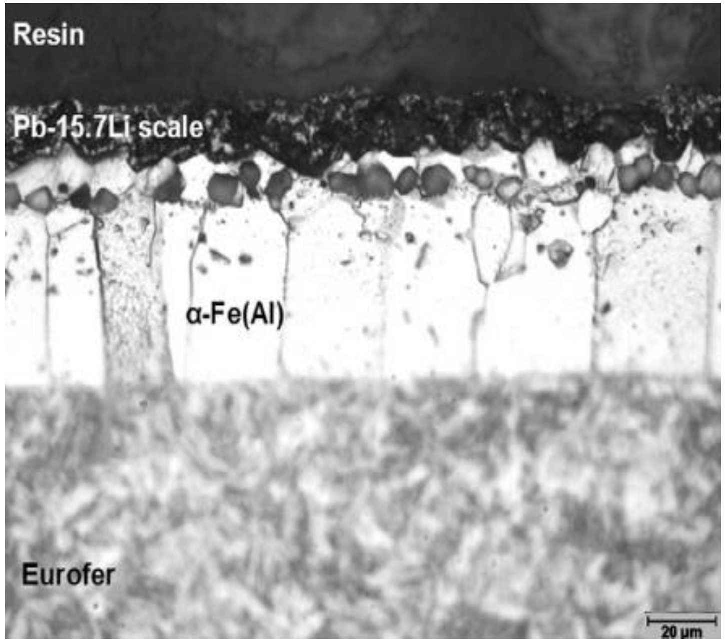

Exposed ECA

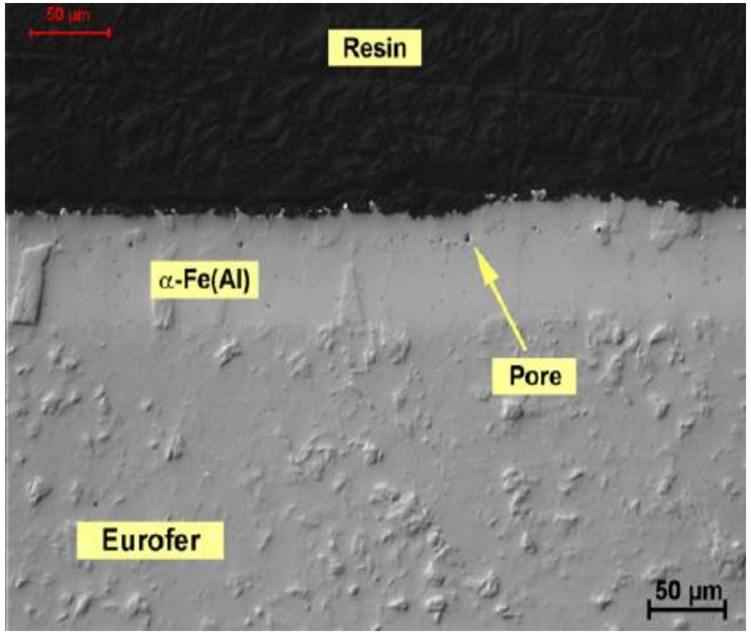

Unexposed ECX

J. Konys et al., *Fusion Engineering and Design* 87 (2012) 1483-1486.
W. Krauss et al., *Journal of Nuclear Materials* 417 (2011) 1233-1236.

Both techniques shown a good barrier behaviour against corrosion (5000h in flowing Pb-17Li at 823K and 0.22m*sec^{-1}).

ECA **PRF** at beginning of life ~ 1000

GESA surface alloying

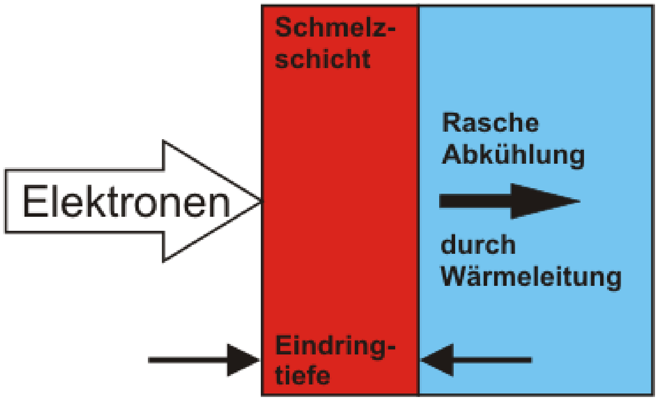

- Eindringtiefe der Elektronen: 10 - 100 μm
- 3 -20 J/cm^2 werden benötig zum Schmelzen
- Rasche Abkühlung durch Wärmeleitung ins Grundmaterial (10^7 -10^9 K/s)
- Effizienter Energieeintrag

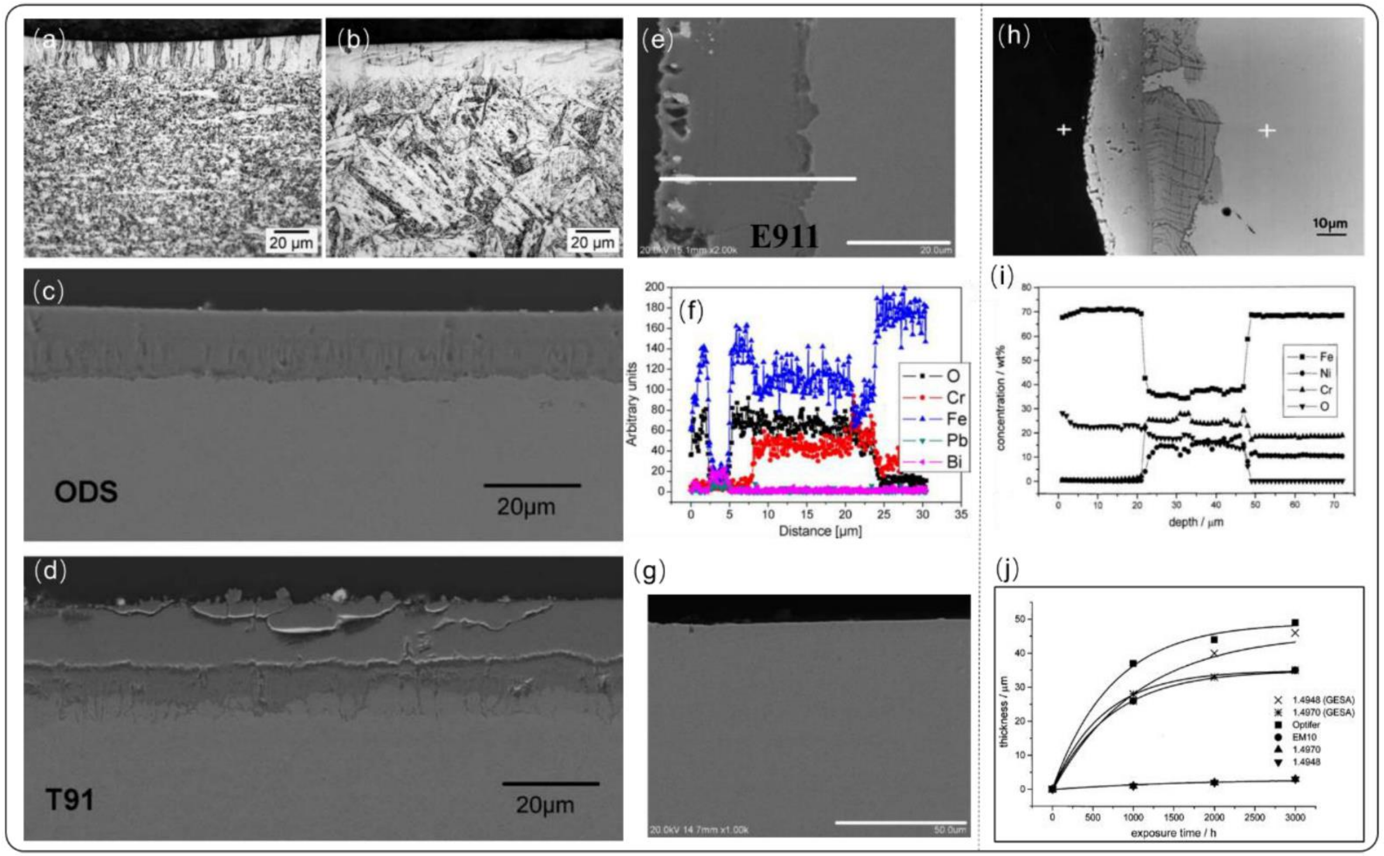

Gepulste Elektronen Strahl Anlage (GESA) treated coatings and corrosion performance. (**a**,**b**) Cross-sectional images of Al-coating on oxide dispersion-strengthened (ODS) and E911. (**c**–**e**) Cross-section images of the Al-coated ODS, T91 and E911 after corrosion test. (**f**) Element distribution of E911after GESA treatment. (**g**) Cross section of ODS with Al alloying. (**h**) Cross section of 1.4948 steel after GESA treatment. (**i**) Element distribution from EDX energy spectrum of EP911. (**j**) Summary of oxide layer thickness at 550 °C in flowing lead [65,66]. ***H. Wang Coatings 2021, 11(3), 364***

ISTITUTO ITALIANO DI TECNOLOGIA

Non equilibrium synthesis of ductile amorphous ceramic coatings for nuclear applications by Pulsed Laser Deposition

Acta Materialia 61 (7), 2662-2670, 2013
Corrosion Science 77, 375-378, 2013
Scientific Reports 6, 33478, 2016
Corrosion Science 124, 80-92, 2017
Acta Materialia 143, 156-165, 2018
Journal of Nuclear Materials 512, 118-125, 2018
Nuclear Fusion 58 (12), 126007, 2018
Journal of Nuclear Materials 516, 160-168, 2019
Fusion Engineering and Design, 2019
Science 366 (6467), 864-869, 2019
Fusion Eng. and Design 158, 111759 3, 2020
Surf. and Coat. Tech. 386, 125491 1, 2020
IAEA TECDOC SERIES, 195, 2020
Fusion Engineering and Design 170, 112521, 2021
NUCLEAR FUSION 61 (1), 2021
Ceramics International 47 (24), 2021
Materials Characterization 178, 2021

fabio.difonzo@iit.it

Nanoceramics for nuclear applications

“Ductile” amorphous ceramics

enhanced → **Mechanical performance**

Ductility, hardness, strength

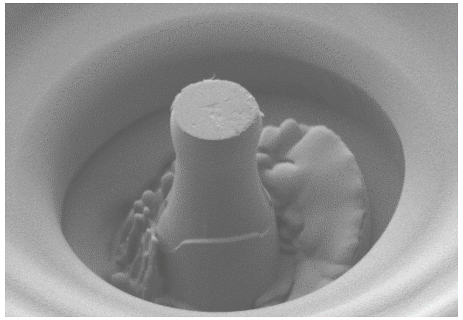

F. Garcia Ferré et al. , SCI REP (2016)
E. Frankberg et al., Science (2019)

enhanced → **$H_2/D_2/T_2$ permeation**

Amorphous structure

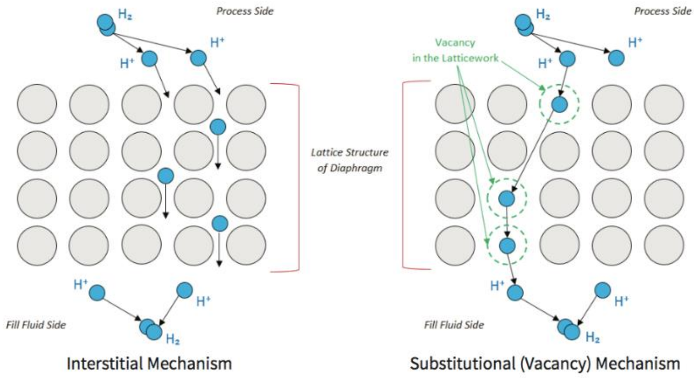

enhanced → **Corrosion resistance**

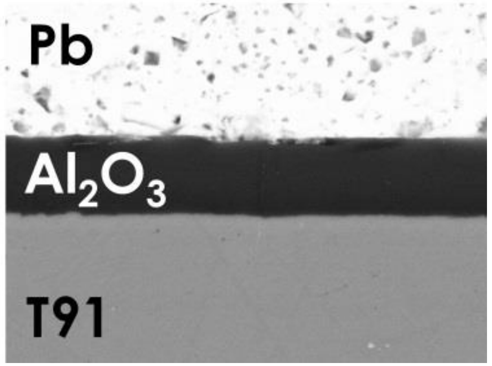

F. Garcia Ferré et al. – CORROS SCI – 2013

enhanced → **Radiation tolerance**

Interstitial emission from GBs

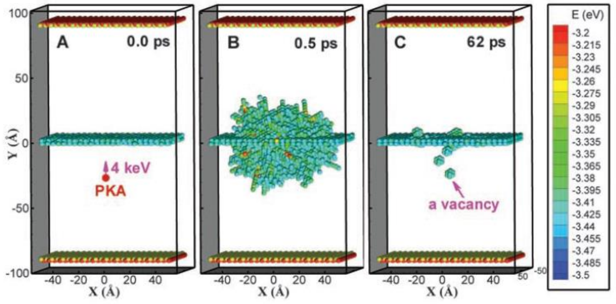

X.M. Bai et al. – Science - 2010

Nanoceramics for nuclear applications

"Ductile" amorphous ceramics

enhanced → enhanced → enhanced → enhanced

Mechanical performance

Ductility, nanohardness

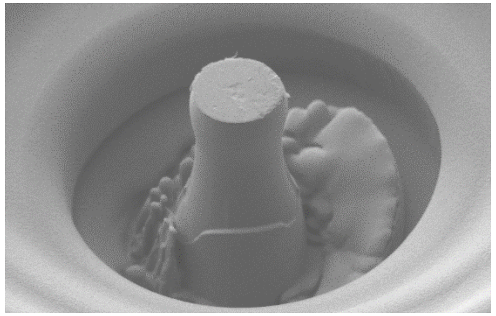

F. Garcia Ferré et al. , SCI REP (2016)
E. Frankberg et al., Science (2019)

$H_2/D_2/T_2$ permeation

Amorphous structure

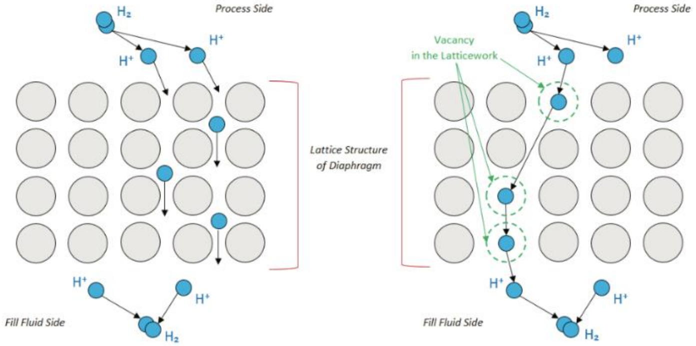

Interstitial Mechanism

Substitutional (Vacancy) Mechanism

Corrosion resistance

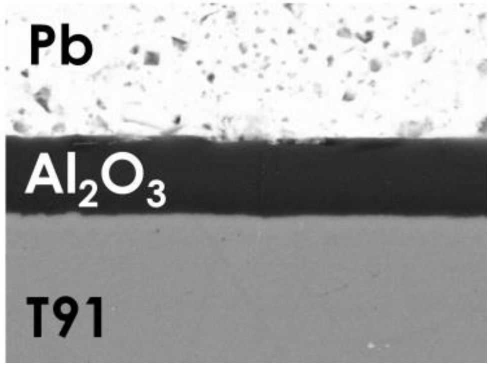

F. Garcia Ferré et al. – CORROS SCI – 2013

Radiation tolerance

Interstitial emission from GBs

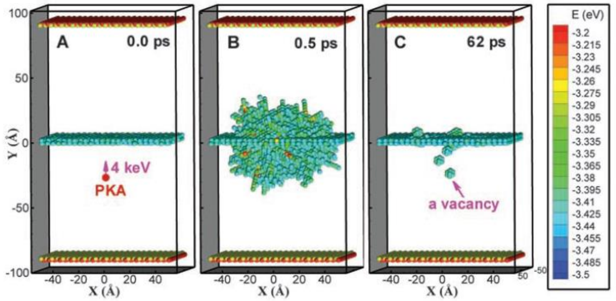

X.M. Bai et al. – Science - 2010

PLD-grown Al_2O_3 nanoceramic coatings

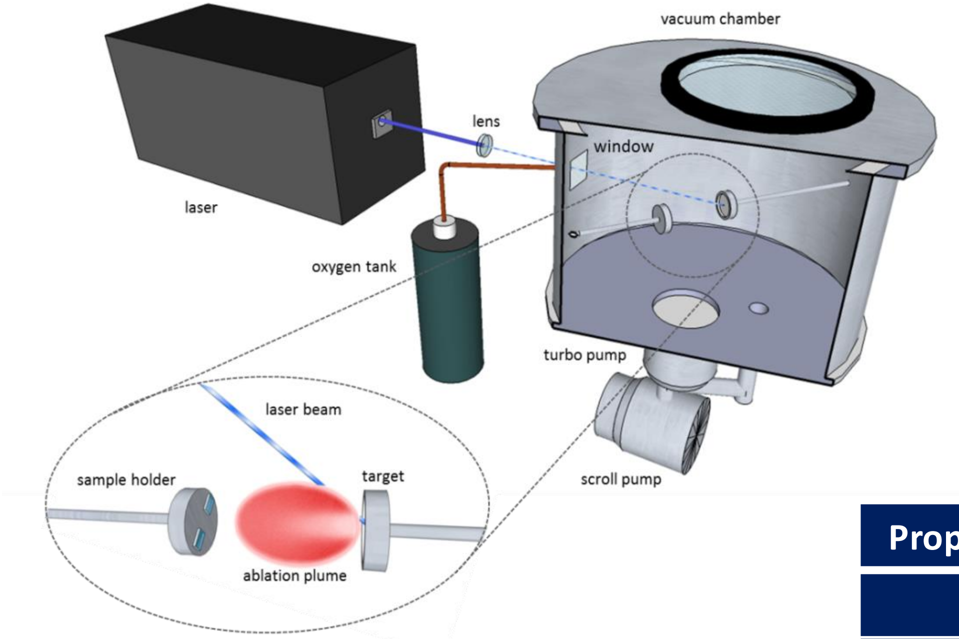

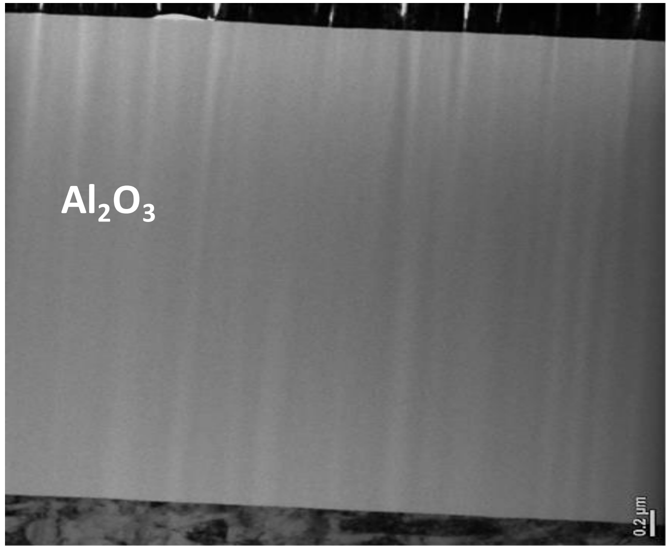

A. Fazi

CHALMERS
UNIVERSITY OF TECHNOLOGY

Property @RT	Sapphire	PLD Al_2O_3	AISI 316L
ν	0,24	0,295 ± 0,025	0,3
E [GPa]	345	193,8 ± 9,9	200
G [GPa]	175	75,5 ± 3,8	80
B [GPa]	240	159,2 ± 11,8	140
H [GPa]	27,8	10,3 ± 1	4
H/E	0,059	0,049 ± 0,007	0,025

- ✓ **amorphous Al_2O_3 is mechanically matched to steels**
- ✓ out-of-equilibrium process, large freedom on chemistry!
- ✓ **density of the amorphous material ≈ crystalline (3.5 g/cm2 for Al_2O_3)**
- ✓ **impervious to gases**
- ✓ **room T process**

H/E parameter index of wear resistance and fracture toughness

F. Garcia Ferré et al. – ACTA MATER – 2013

Mechanical behaviour of PLD-grown Al_2O_3

- **Nanoindentation Tests**

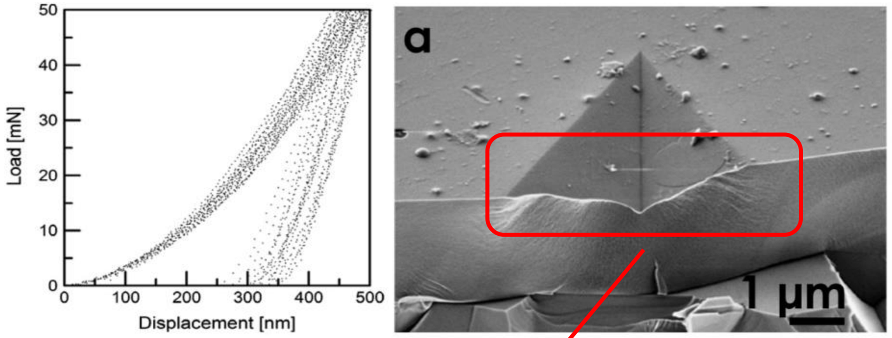

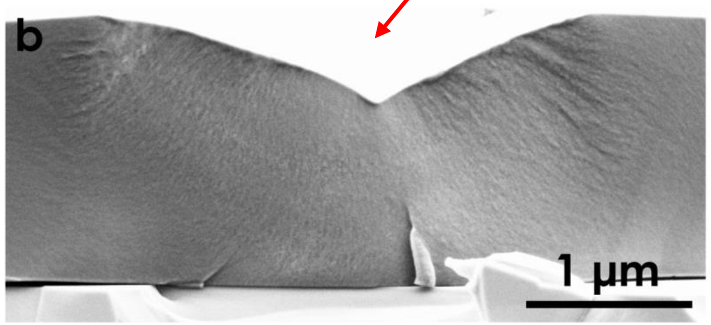

metal-like behavior under plastic strain

Plastic work 62%

- **Nanoscratch Tests**

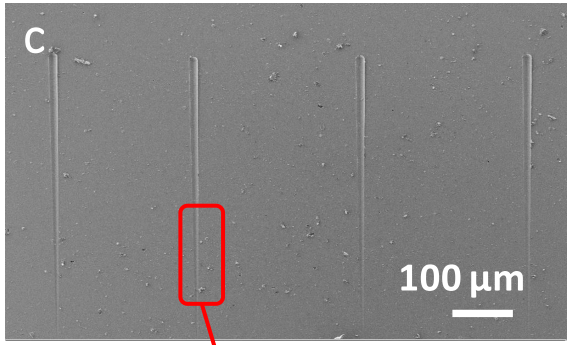

No delamination
No critical load

Strong interfacial bonding

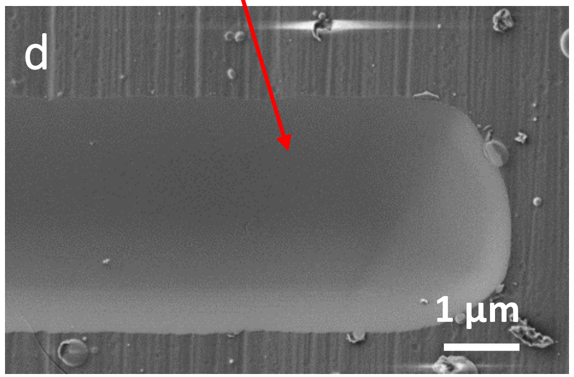

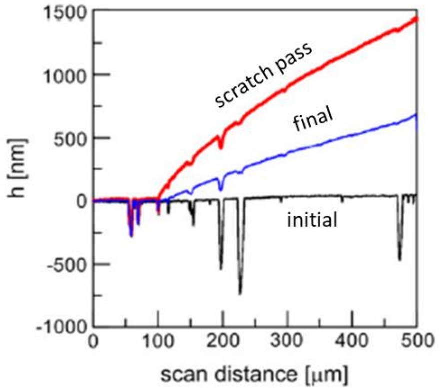

strong interfacial bonding

F. Garcia Ferré et al. – ACTA MATER – 2013

Ductility at the nanoscale of PLD Al_2O_3

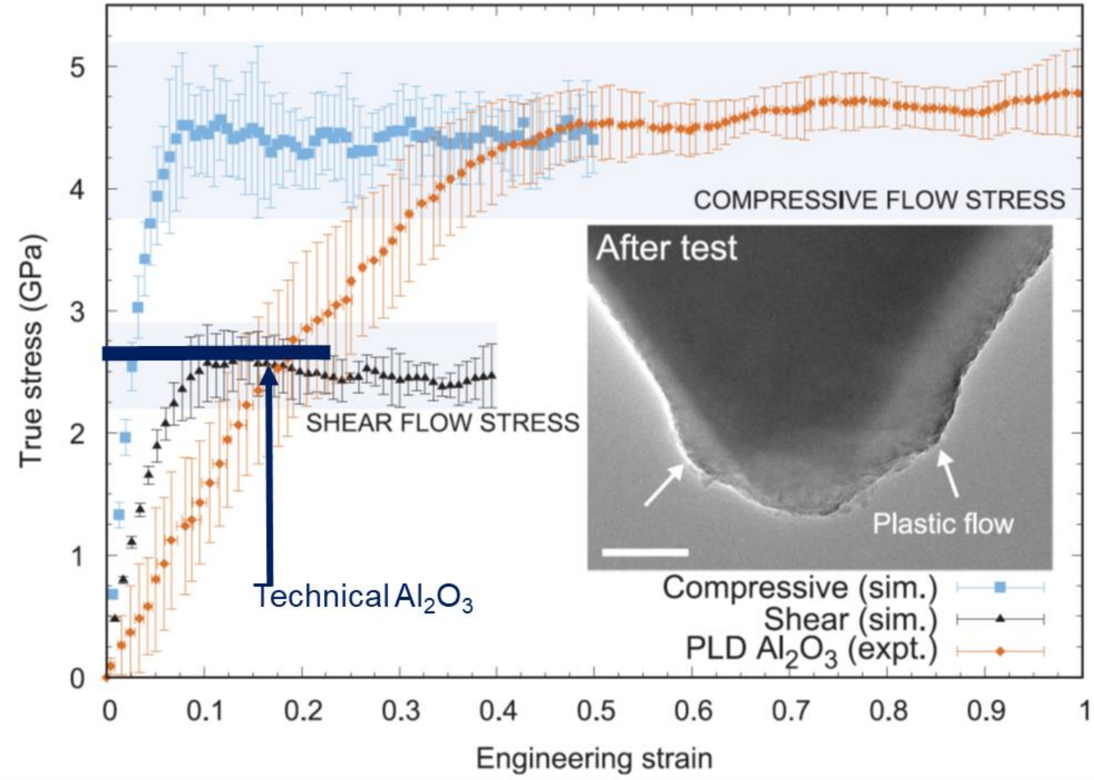

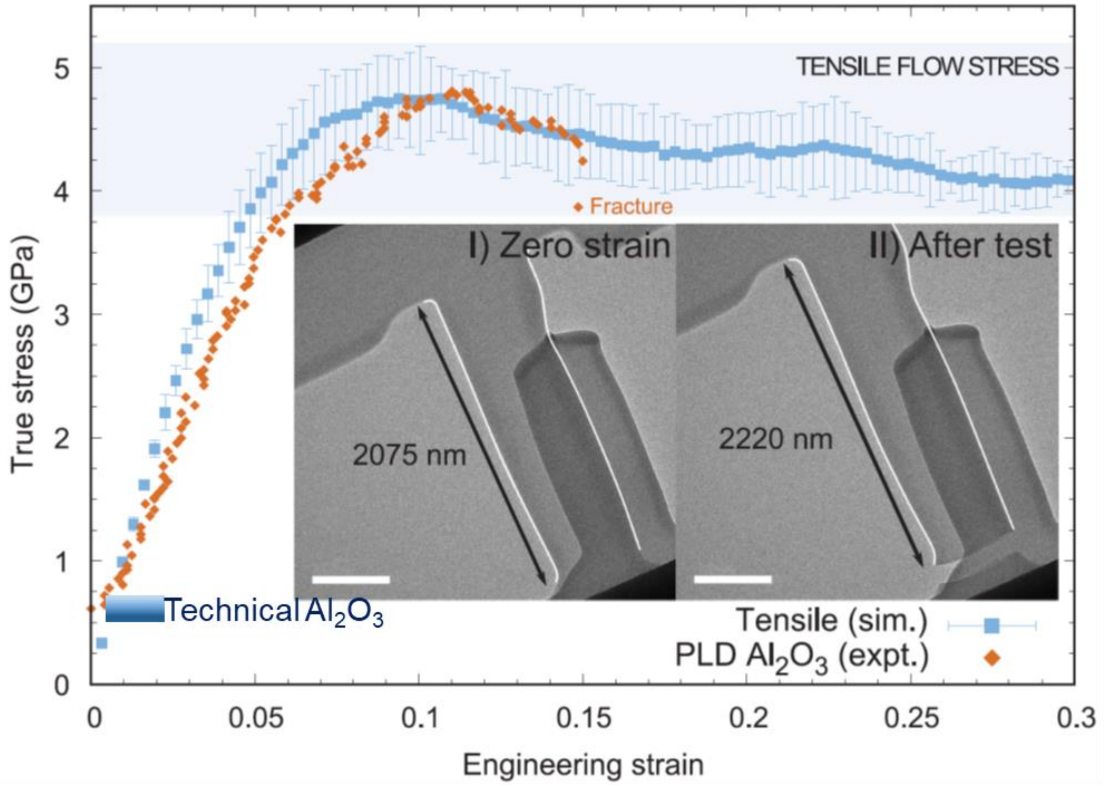

In situ TEM results:

-compression: 100% deformation

-tensile: 15 % total elongation, 7% plastic deformation to failure

E. Frankberg et al. Science 864-869, 2019

Nanoceramics for nuclear applications

"Ductile" amorphous ceramics

enhanced

enhanced

enhanced

enhanced

Mechanical performance

Ductility, hardness, strength

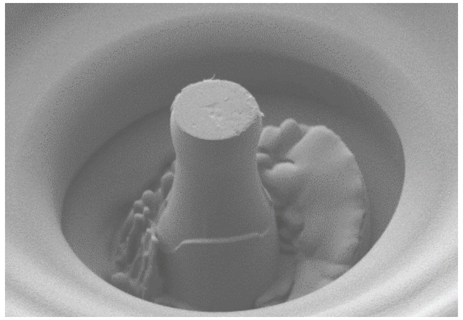

F. Garcia Ferré et al. , SCI REP (2016)
E. Frankberg et al., Science (2019)

$H_2/D_2/T_2$ permeation

Amorphous structure

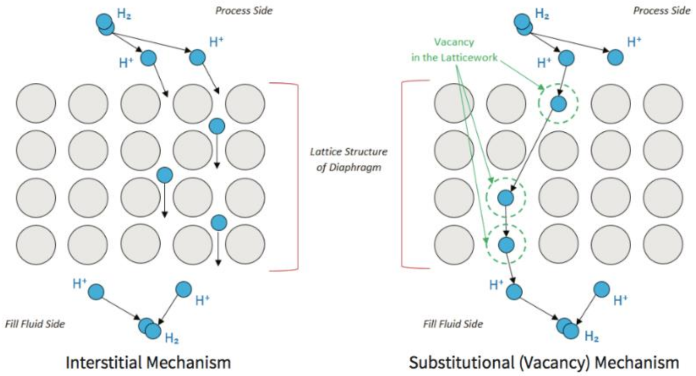

Corrosion resistance

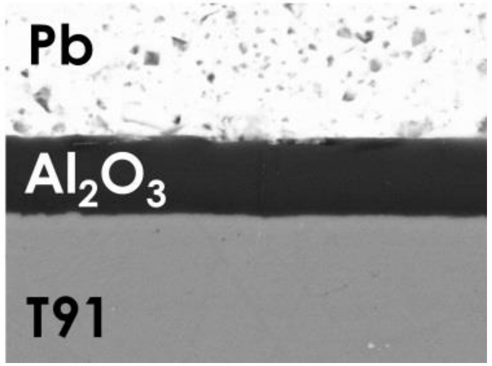

F. Garcia Ferré et al. – CORROS SCI – 2013

Radiation tolerance

Interstitial emission from GBs

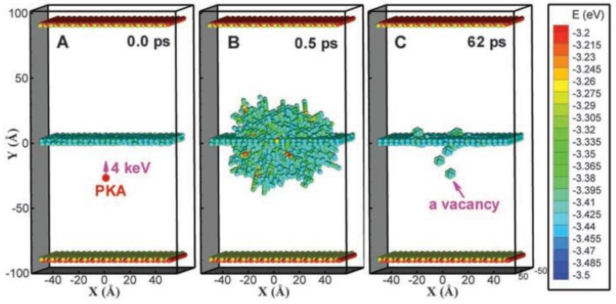

X.M. Bai et al. – Science - 2010

O_2 permeation barrier

316L plate

coating

annealed 2h @ 1000°C in air

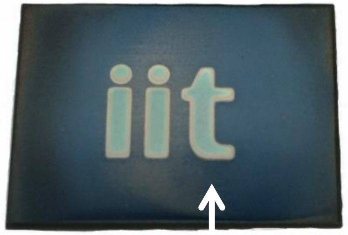

coating

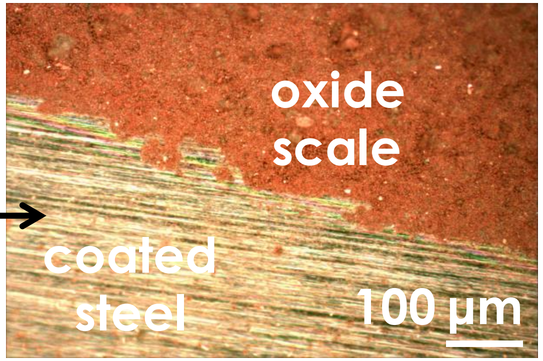

fabio.difonzo@iit.it

Dielectric and permeation barrier properties

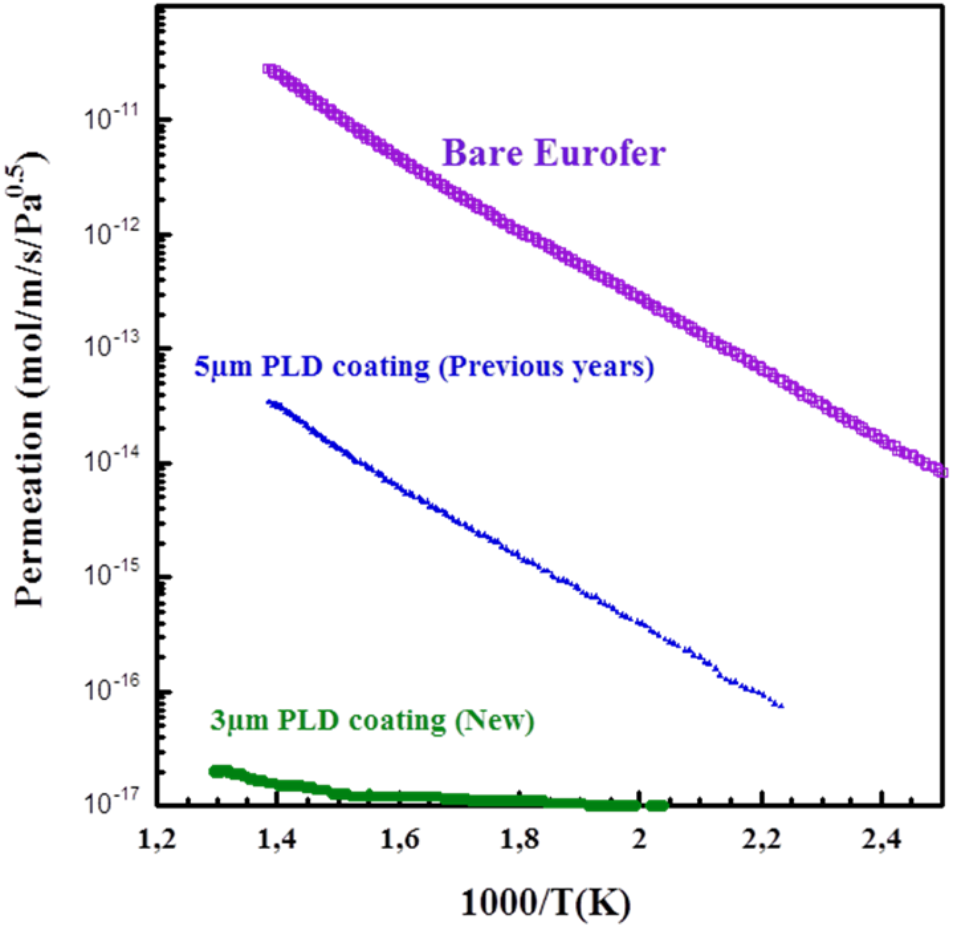

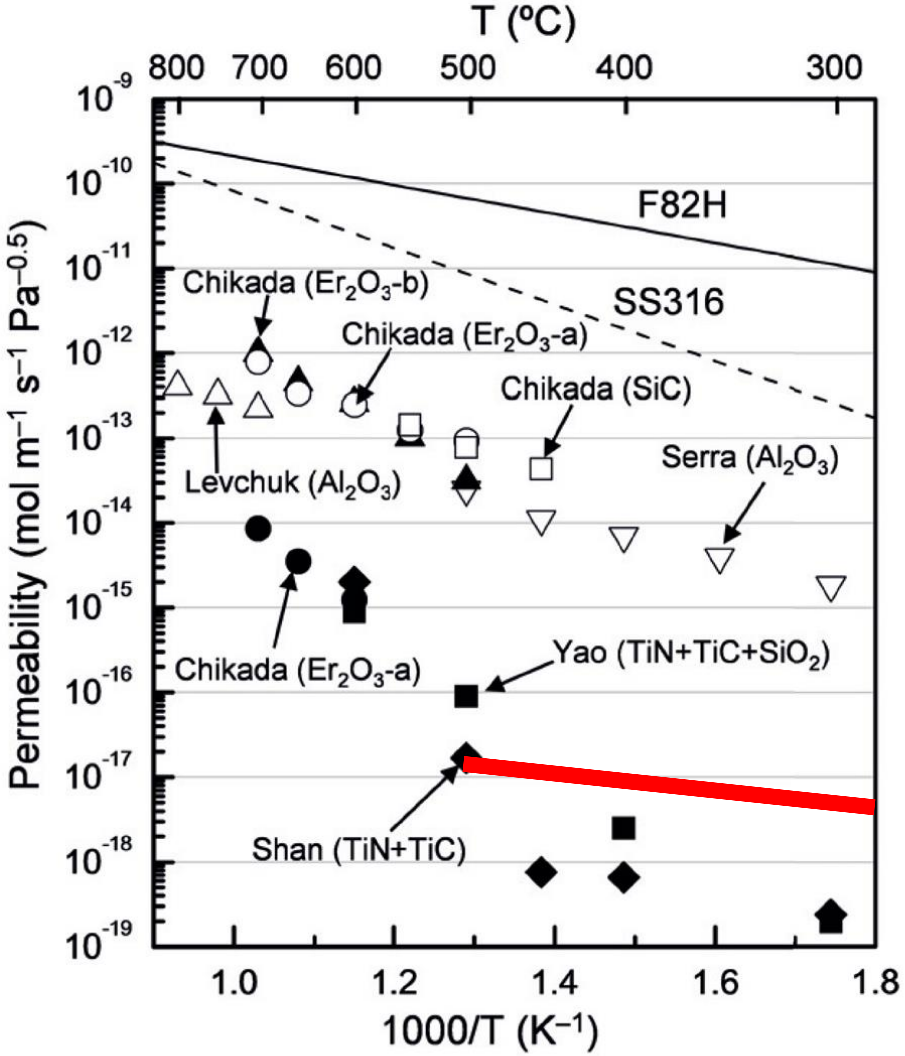

$$PRF = \frac{J^D_{Bare}}{J^D_{Coated}} > \mathbf{10^5\ @\ 450\ °C}$$

fabio.difonzo@iit.it

Nanoceramics for nuclear applications

"Ductile" amorphous ceramics

enhanced

Mechanical performance

Ductility, hardness, strength

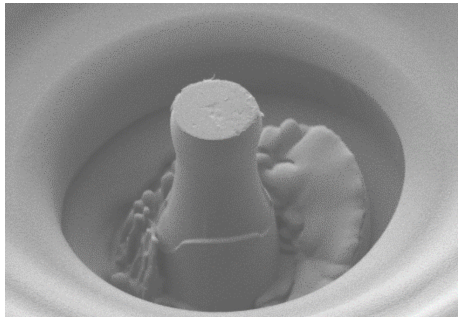

F. Garcia Ferré et al. , SCI REP (2016)
E. Frankberg et al., Science (2019)

$H_2/D_2/T_2$ permeation

Amorphous structure

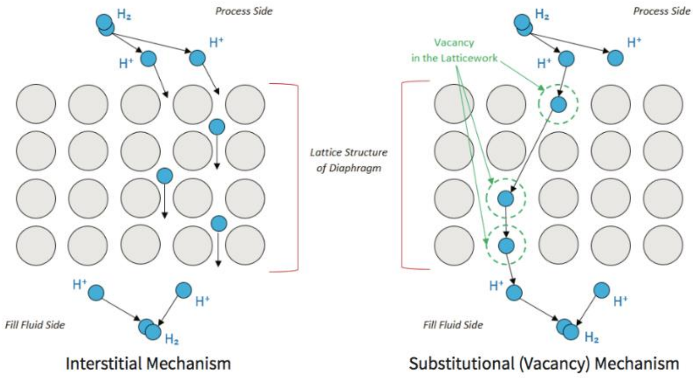

Corrosion resistance

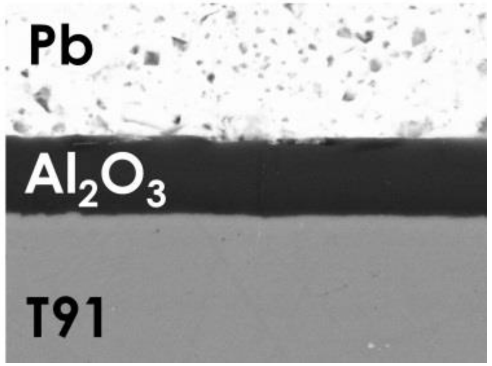

F. Garcia Ferré et al. – CORROS SCI – 2013

Radiation tolerance

Interstitial emission from GBs

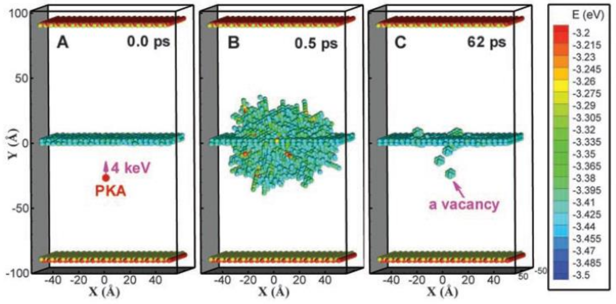

X.M. Bai et al. – Science - 2010

ISTITUTO ITALIANO
DI TECNOLOGIA

10 years of corrosion experiments

Stagnant lead (LFR)
- 500 h @ 550 °C
- No oxygen control

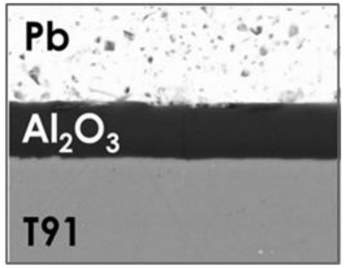

Garcia Ferrè F. et al.,
Corr. Science, 2013

Stagnant lead (LFR)
- 10˙000 h @ 550 °C
- 10^{-3} - 10^{-8} wt.% O_2

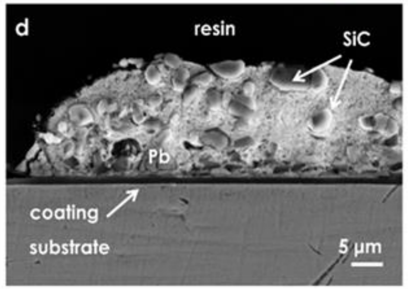

Garcia Ferrè F. et al.,
Corr. Science, 2017

Stagnant lead (LFR)
- 1˙000 h @ 550 °C
- pre-irradiated coating

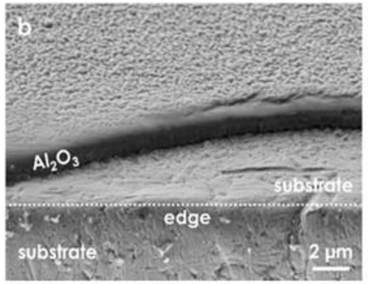

Garcia Ferrè F. et al.,
Corr. Science, 2017

Flowing lead (LFR)
- 200 h @ 525 °C
- 10^{-4} wt.% O_2

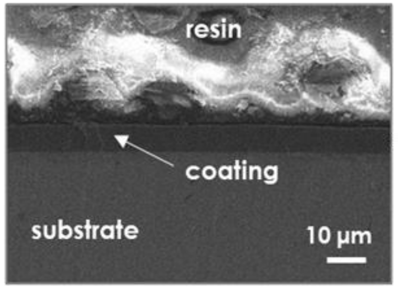

Vanazzi M. et al.,
IAEA technical report, 2021

Stagnant Pb-55Bi (LFR)
- 1˙000 h @ 500 °C
- 10^{-10} wt.% O_2

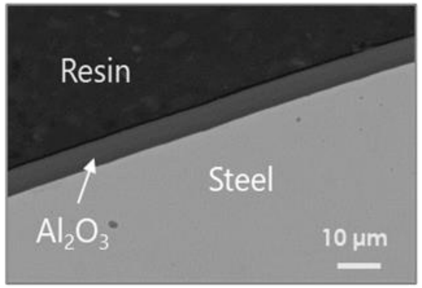

E. Charalampopoulou, et al.,
Mat. Char., 2021

Stagnant Pb-16Li (BB)
- 8˙000 h @ 550 °C
- 10^{-8} wt.% O_2

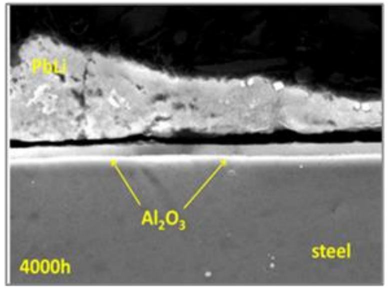

Iadicicco D. et al.,
Fus. Des. and Eng., 2019

Li_4OSi_4 pebbles (BB)
- 730 h @ 800 °C
- Pebbles bed system

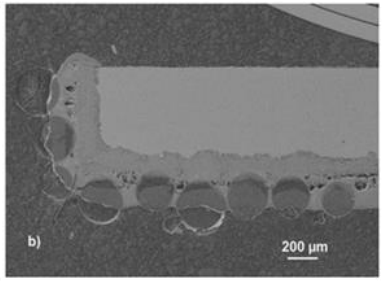

Hernandez T. et al.,
J. of Nuc. Mat., 2019

Corrosion tests in static Pb-16Li

➢ **Stagnant LLE Corrosion Test on alumina-coated EU-97 steel (**collaboration with **ENEA)**

- **Test temperature 550 °C** - up to **8˙000 hours** - **O_2 %** monitored (**dissolutive** @ **10^{-8} wt.% regime**)

UNPROTECTED sample

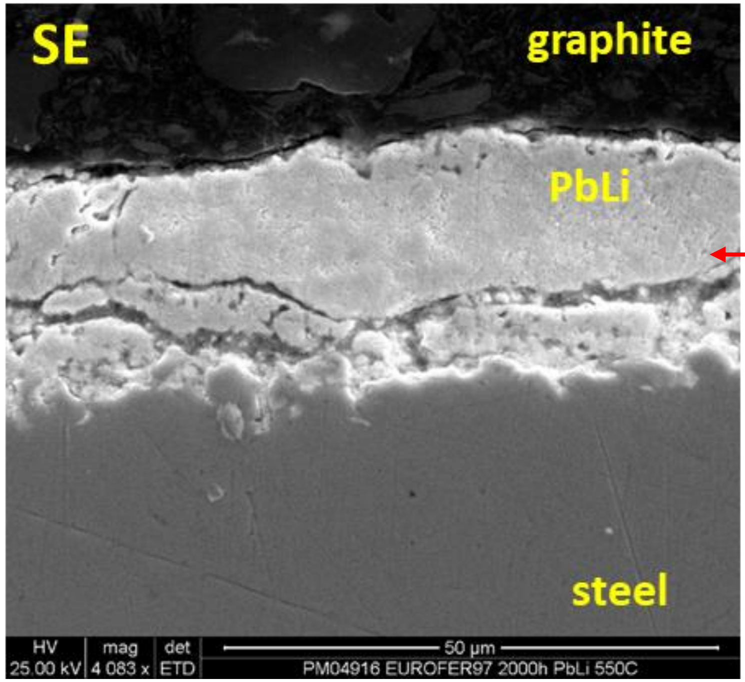

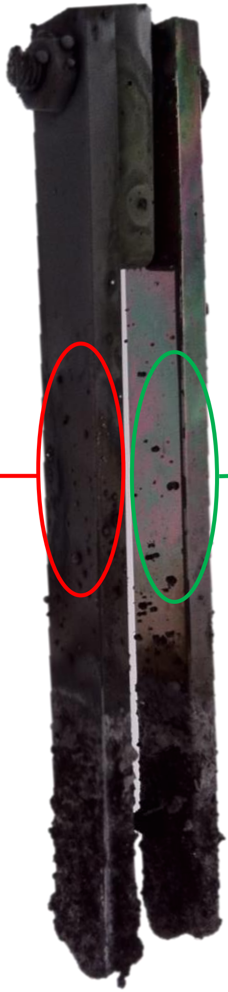

COATED sample

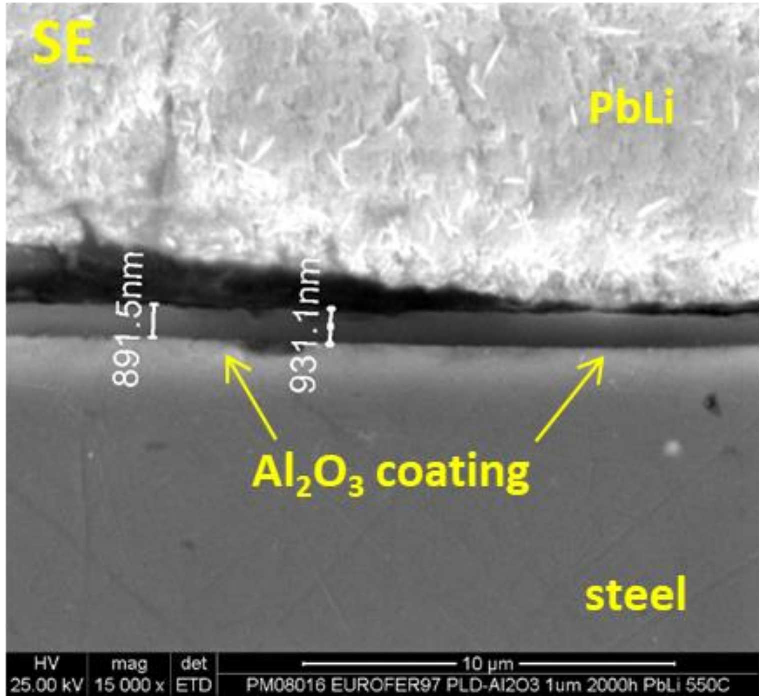

fabio.difonzo@iit.it

Thermodynamics of Al_2O_3 in PbLi

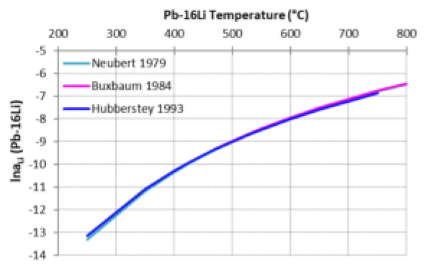

a_{Li} activity from Hubbestey 1993
$\Delta G°_f$ Li_2O, Al_2O_3, $LiAlO_2$ from Barin
$\Delta G°_f$ $LiAl_5O_8$ from NBS table

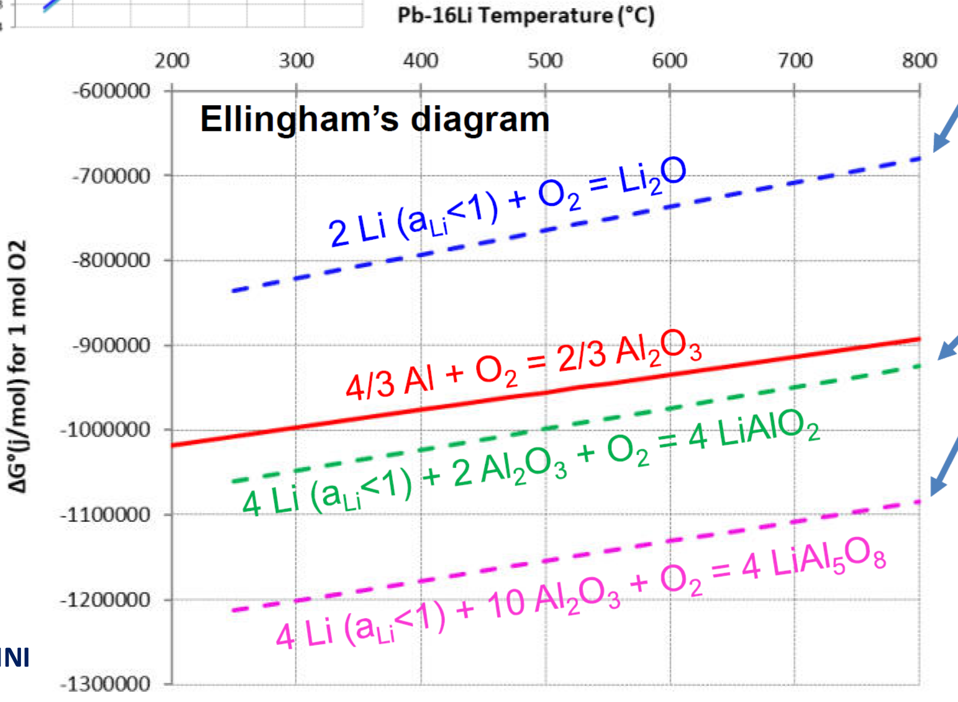

Credits to S. BASSINI from ENEA

- Al2O3 is stable in liquid PbLi eutectic thanks to the low Li activity (Hubberstey 1997).
- Experimentally, LiAlO2 formation occurred in PbLi eutectic on crystalline Al2O3 layer at 800°C after 1000h (Pint 2008).
- LiAlO2 formation was observed on crystalline alumina powder in PbLi exposed to air at 550°C after 48h. No formation under vacuum, slow kinetics under flowing inert gas (Jain 2014).
- LiAl5O8 and LiAlO2 formation from Al2O3 is thermodynamically favored in PbLi. LiAl5O8 is more stable, in agreement with our experiments which shows about LiAl5O8 formation.
- Effect of kinetics should be investigated: likely LiAlO2 formation is promoted at high temperature and with source of oxygen (air or inert gas flowing) whereas LiAl5O8 is formed at lower temperature with minor oxygen availability (e.g. inert gas overpressure in our experiments).

Nanoceramics for nuclear applications

“Ductile” amorphous ceramics

enhanced

enhanced

enhanced

enhanced

Mechanical performance

Ductility, hardness, strength

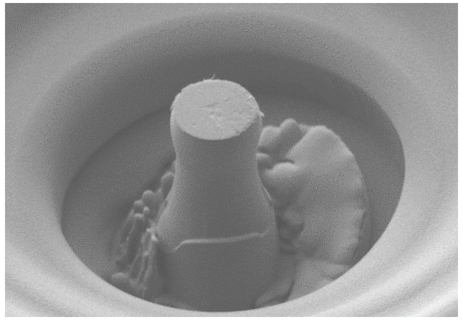

F. Garcia Ferré et al. , SCI REP (2016)
E. Frankberg et al., Science (2019)

$H_2/D_2/T_2$ permeation

Amorphous structure

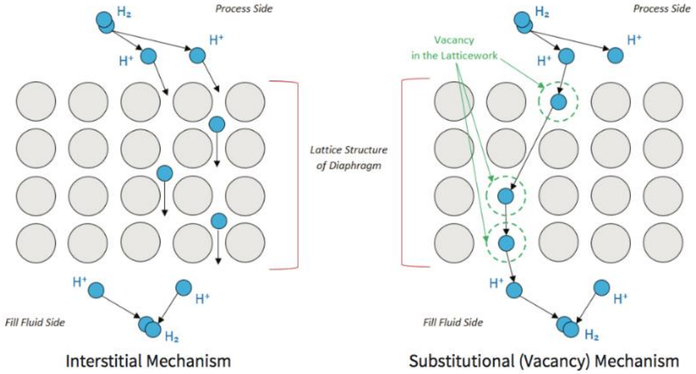

Corrosion resistance

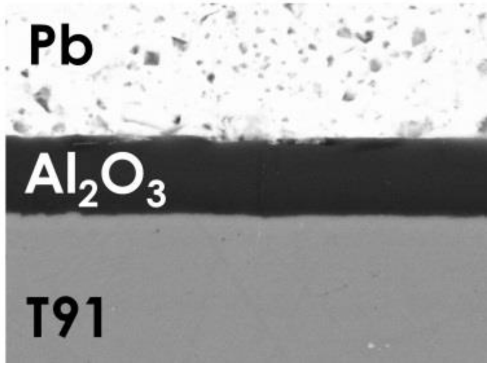

F. Garcia Ferré et al. – CORROS SCI – 2013

Radiation tolerance

Interstitial emission from GBs

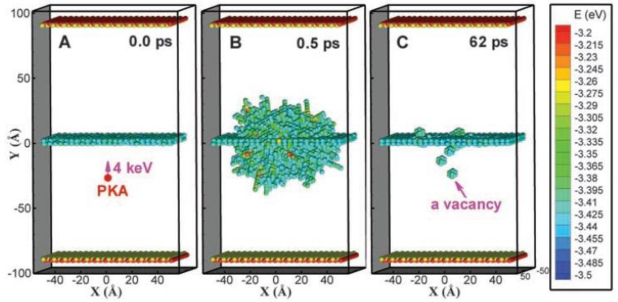

X.M. Bai et al. – Science - 2010

Model of evolution

moderate dpa

ultra-fine nanoceramic
GB-driven deformation
highest fracture toughness

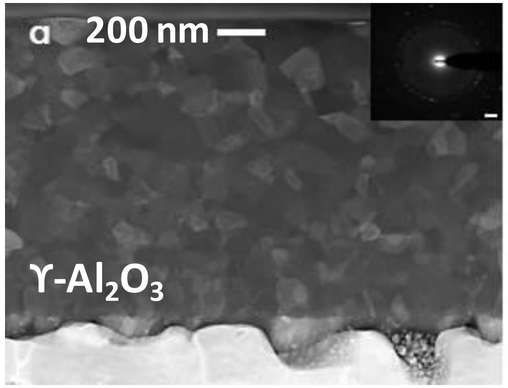

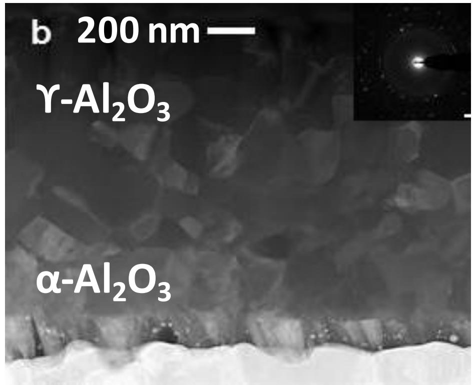

high dpa

fine nanoceramic
GB-driven deformation
sub-linear grain growth

pristine

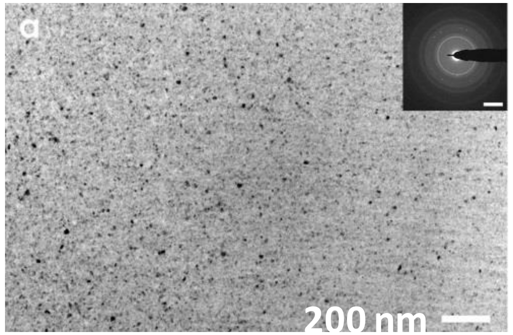

bi-phase nanocomposite
shear banding
highest fracture strength

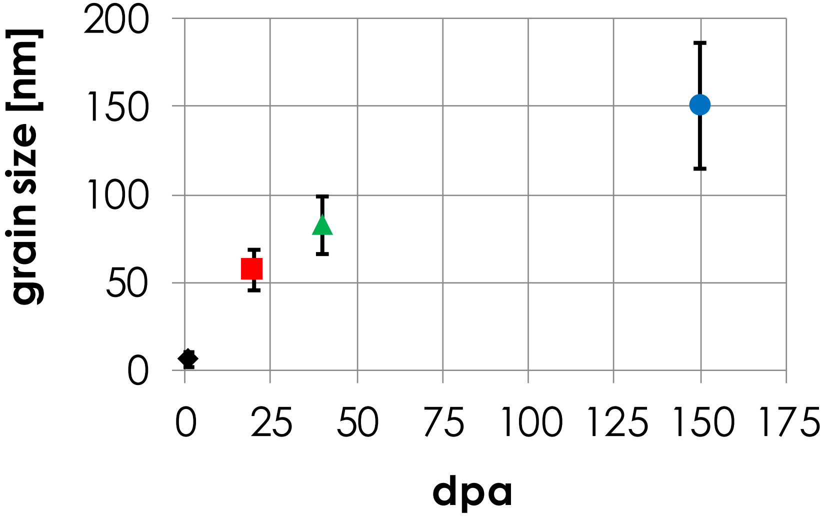

Sublinear grain growth

end-of-life dpa

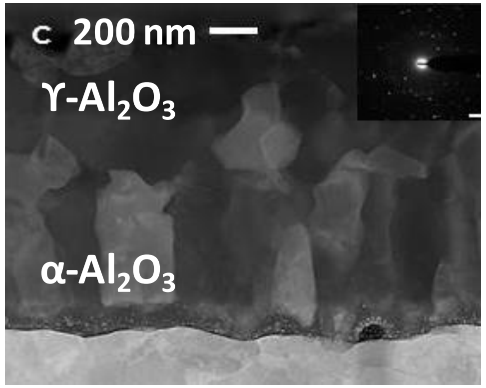

nanoceramic
GB-driven deformation
highest stiffness

F. Garcia Ferré et al. – SCI REP – 2016

Heavy ion irradiation (Au + W): swelling at 150 dpa

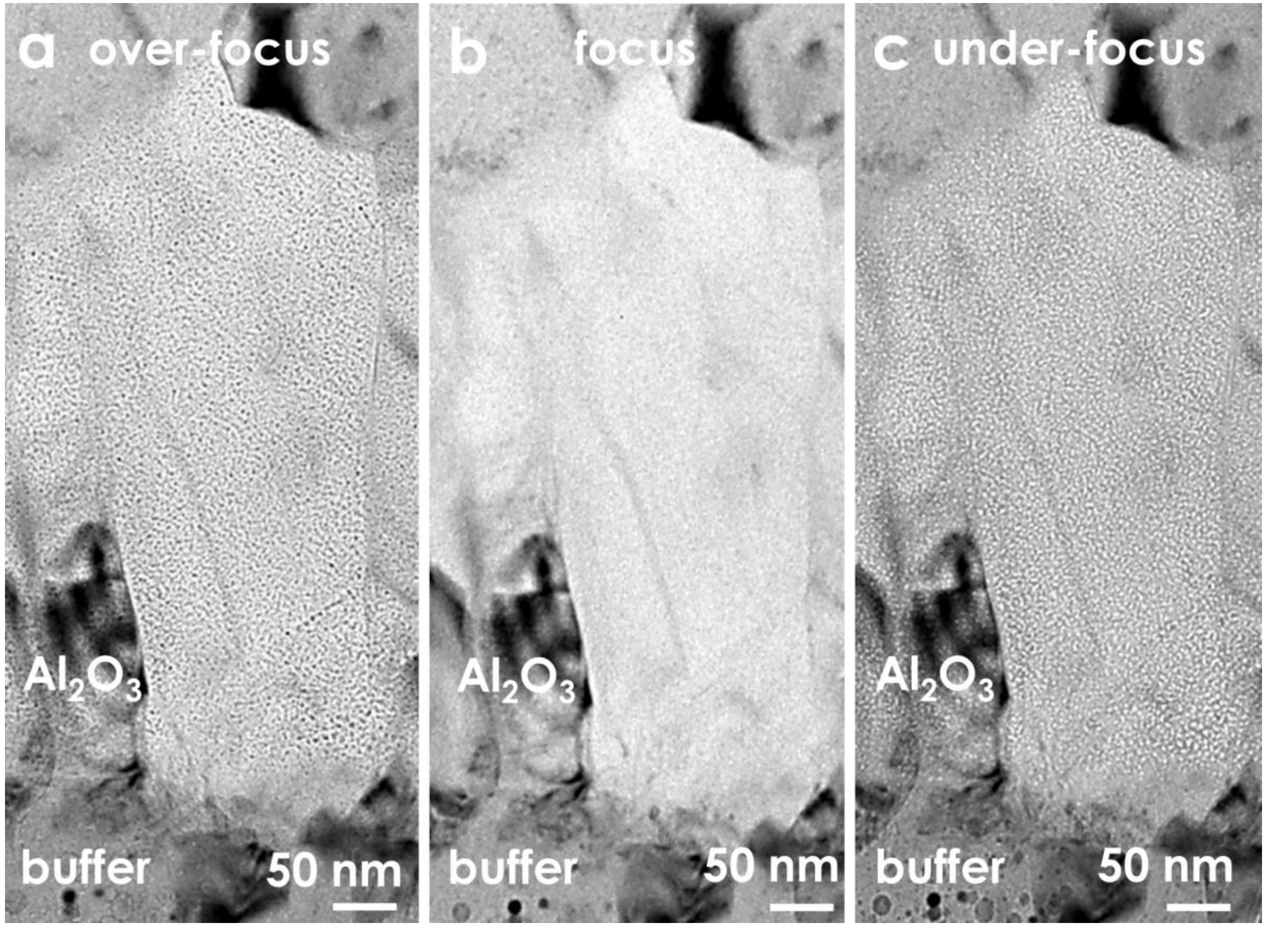

- **Large number of small voids, only in a monolayer of grains, at the interface with the buffer layer**
- **These grains are alpha-alumina. All the other grains are gamma-alumina**

F. Garcia Ferré et al. – SCI REP – 2016

fabio.difonzo@iit.it

Heavy ion irradiation (Au + W): nanoimpact

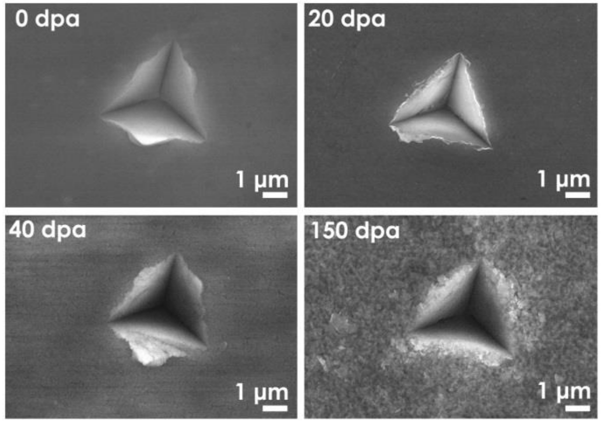

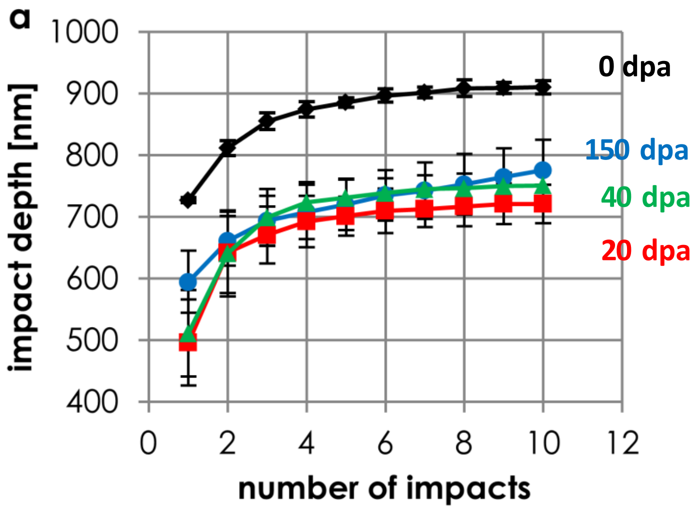

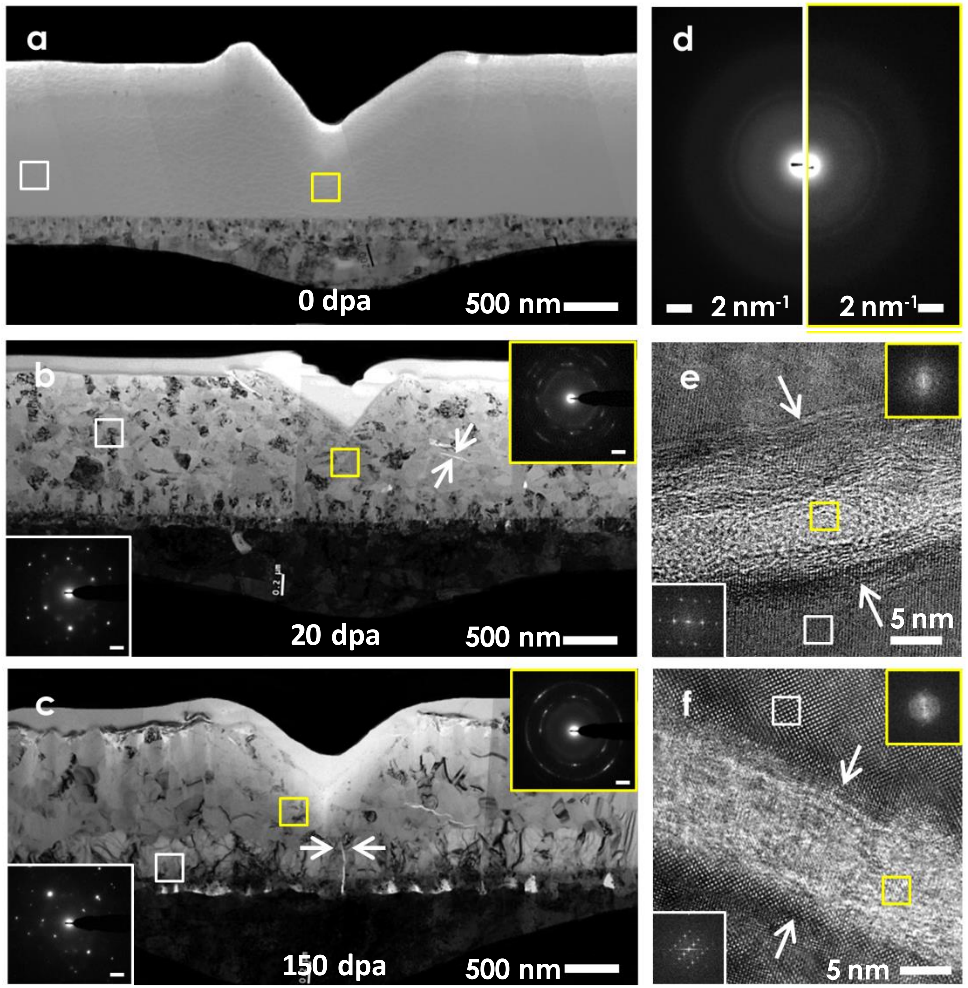

Shear banding

Lattice bending & localized shear amorphization

Lattice bending & localized shear amorphization

Impact energy is dissipated more efficiently in irradiated samples

F. Garcia Ferré et al. – SCI REP – 2016

ISTITUTO ITALIANO
DI TECNOLOGIA

Conclusions

fabio.difonzo@iit.it

Conclusions

➢ Qualification tests for Lead Fast Reactor and Breeding Blanket applications: a follow up

- Corrosion tests in **static/fluent Pb**, **static LBE** and **LLE** up to **10˙000 hours**
- Combined tests of **permeation** with **D_2 under electron irradiation**
- **Engineering of mechanical response** in nano-ceramic coatings

➢ Evolution of barrier coatings under irradiation: design and understanding

- **Role of the irradiation parameters** on the material changes (ion type, T, flux, etc.)
- Formulation of a **structural/mechanical model** to **predict the evolution of alumina**
- **Control of the crystallization** by **chemical doping: improved performance**

➢ Future development for the technological licensing

- Continuation of **relevant tests** (corrosion, permeation, etc.) with an **integrated approach**
- Collection of **ions VS neutrons experiment results** to support the present data
- **Towards high entropy stabilization of ductile amorphous oxides under irradiation**

fabio.difonzo@iit.it

Acknowledgements & Funding Sources

Collaborators

ISTITUTO ITALIANO DI TECNOLOGIA

Luca Ceseracciu
Rosaria Brescia
Mirko Prato
Guglielmo Lanzani

Previous members:

Francisco Garcia Ferré
Erkka Frankberg
Matteo Vanazzi
Daniele Iadicicco

ENEA – Ente per le Nuove tecnologie, l'Energia e l'Ambiente

Serena Bassini
Marco Utili
Mariano Tarantino
Pietro Agostini

Politecnico di Milano

Marco Beghi

JANNUS

Heavy ion irradiations
CABET Celine
LOYER-PROST Marie

Ciemat – Centro de Investigaciones Energéticas, Medioambientales y Tecnológicas

Teresa Hernandez

TAMPERE UNIVERSITY OF TECHNOLOGY

Gaurav Mohanty, Janne Kalikka,
Erkka Frankberg, Turkka Salminen,
Erkki Levänen

NTNU – Norwegian University of Science and Technology

Jaakko Akola

Argonne NATIONAL LABORATORY

Dr. Jinh Hu
Dr. Wei-Ying Chen
Dr. Meimei Li

INSA – INSTITUT NATIONAL DES SCIENCES APPLIQUÉES LYON

Karine Masenelli-Varlot

Narodowe Centrum Badań Jądrowych
National Centre for Nuclear Research
ŚWIERK
Instytut kategorii A+, JRC collaboration partner

Agata Zaborowska
Łukasz Kurpaska

fabio.difonzo@iit.it

Acknowledgements & Funding Sources

Financial support

Ministero dello Sviluppo Economico

EERA European Energy Research Alliance JPNM
JOINT PROGRAMME ON NUCLEAR MATERIALS

EUROfusion

NSUF Nuclear Science User Facilities

GEMMA

TRANSAT
TRANSversal Actions for Tritium

IL TROVATORE

First Prize at SOFT 2020 Innovation Prize

ISTITUTO ITALIANO DI TECNOLOGIA
CENTER FOR NANOSCIENCE AND TECHNOLOGY

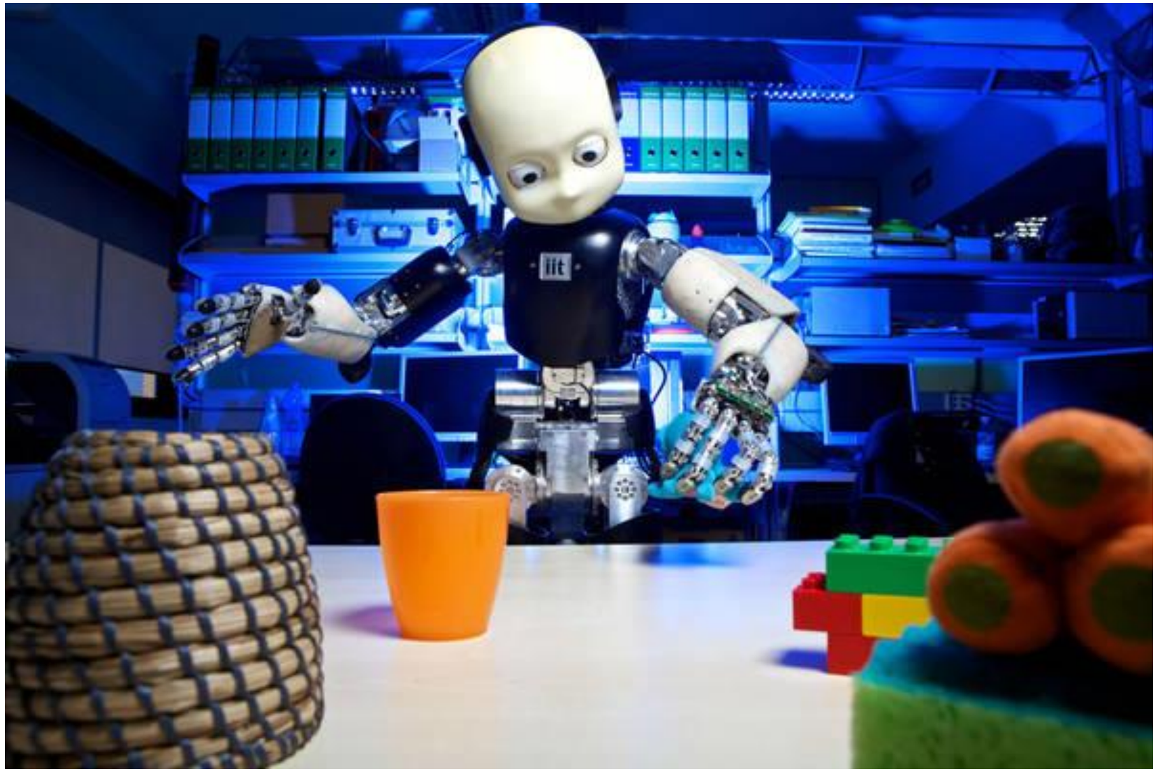

Thank You
for your attention!

fabio.difonzo@iit.it